INTERNATIONAL GEOLOGY REVIEW
https://doi.org/10.1080/00206814.2020.1795734

Taylor & Francis
Taylor & Francis Group

Crustal fluid contamination in the Bushveld Complex, South Africa: An analogue for subduction zone fluid migration

Erin Benson[a], James A. D. Connolly[b] and Alan E. Boudreau[a]

[a]Div. Earth and Ocean Science, Duke University, 27708, Durham, NC, USA; [b]Department of Earth Sciences, Swiss Federal Institute of Technology, Zurich, Switzerland

ABSTRACT

Crystallization of the 2.06 Ga Bushveld magma formed a 9 km (maximum) sequence of ultramafic and mafic rocks that generated a large volume of country fluid as it thermally metamorphosed a 3+ km section of previously unaltered underlying sedimentary rocks of the Transvaal sequence – a geometry similar to that seen as subducting lithospheric slabs are heated by overlying mantle rocks. The presence of a diatreme (breccia pipe) and other large, pipe-like features in the Bushveld Complex located proximal to diapiric upwelling of the basement rocks suggest that overpressured fluids generated during dehydration of the footwall sediments are focused by the diapiric structures such that the country fluids rapidly penetrate the Bushveld rock. A re-examination of existing stable and radiogenic isotopic evidence is consistent with contamination of Main Zone magmas by 1–2% country fluid. Numeric modelling of the footwall dehydration similarly shows that most of the country fluids will be confined to pipe-like channels as it percolates into the Bushveld sill. Modelling also suggests that the maximum extent of the metamorphic aureole was reached at about the same time that the Main Zone began to crystallize. It is proposed that rapid inflation of the Bushveld sill induced the sudden and catastrophic expulsion of overpressured country fluids to both generate the diatreme and contaminate the Main Zone magma, resulting in the Main Zone enrichment in crustal stable and radiogenic isotopic signatures (Sr, Nd, O and others). By analogy, it is also suggested that hydration melting in the mantle wedge is episodically driven by similar sudden influxes of slab fluids that are able to retain their geochemical and isotopic character by rapid channelled influx. This can be aided by flow focusing at diapirs structures at the upper slab-mantle contact.

ARTICLE HISTORY
Received 11 November 2019
Accepted 11 July 2020

KEYWORDS
Bushveld complex; subduction; slab fluids

1. Introduction

The 2.06 Ga (Walraven 1988) Rustenburg Layered Series of the Bushveld Complex of the Republic of South Africa (hereafter simply referred to as the Bushveld Complex) is the world's largest layered intrusion, with area estimated to be >90,000 km^2 and a volume exceeding 450,000 km^3 (*e.g.*, Finn *et al*. 2015; Figure 1). In part because the intrusion is economically significant (hosting significant platinum-group element, chrome and vanadium deposits), many studies have been undertaken of Bushveld formation. The Bushveld Complex exhibits a broad stratigraphic trend upwards to more fractionated rock compositions (*e.g.*, Eales and Cawthorn 1996; Maier *et al*. 2000; Figure 2). Early studies of Bushveld formation primarily relied on these compositional trends and considered the Bushveld to have formed by the continuous recharge and fractional crystallization of a single parent magma. Since then, observations of stratigraphic isotopic changes have led to a number of more complex models, including partial melting of enriched mantle or assimilation of lower and/or upper crustal rocks during emplacement, some of which resultant magma may have different liquid lines of descent (*e.g.* Irvine 1977; Von Gruenewaldt *et al*. 1985; Hatton and Sharpe 1989; Harmer *et al*. 1995; McCandless *et al*. 1999; Maier *et al*. 2000; Harris *et al*., 2005; VanTongeren 2018). For example, it is envisioned that the Sr isotopic change observed between the Main Zone and underlying rocks was the result of the introduction of a large volume of extensively contaminated Main Zone magma and a significant expansion of the Bushveld chamber (Kruger 2005).

Although a number of studies have called upon contamination by upper crustal/roof rocks (e.g., Kruger 2005; Harris *et al*. 2005), the possibility that at least some of the large-scale isotopic variation is the result of *in situ* contamination of the Bushveld magma by crustal fluids has not been seriously explored outside of local contamination or late-stage modification of the original mineral assemblage. However, other areas of study have explored the impact of crustal fluid contamination of magma or its source rock. For instance, evidence from subduction zone magmas illustrates that crustal fluids can clearly affect the isotopic

CONTACT Erin Benson erin.k.benson@duke.edu Div. Earth and Ocean Science, Duke University, Durham, NC, 27708, USA

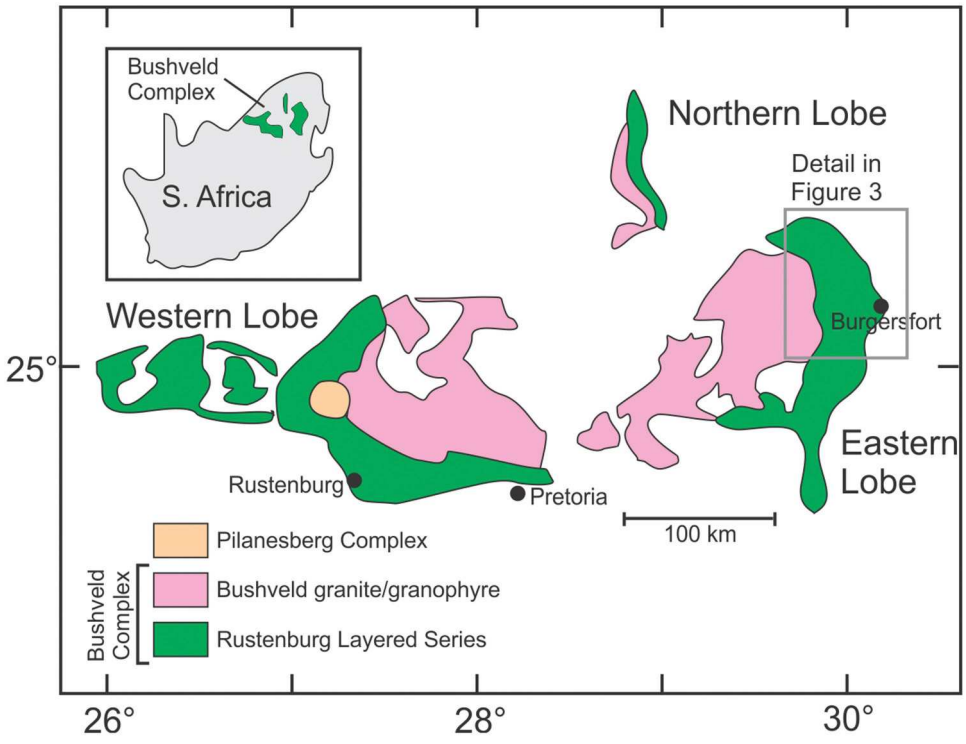

Figure 1. Location map of the Bushveld Complex, Republic of South Africa, showing the three major parts of the Bushveld, the Western Eastern and Northern Bushveld lobes. The location of the detail of the Eastern lobe shown in ***Figure 3*** is also noted.

character of a mantle magma (*e.g.*, Nohda and Wasserburg 1981; Ito and Stern 1986; Shaw *et al*. 2008; Woodhead *et al*. 2012). Furthermore, investigations into fluid contamination at various intrusions often rely heavily on isotopic compositions to differentiate between fluid alteration and crustal assimilation (e.g., Leeman and Hawkesworth 1986; Hildreth *et al*. 1991).

This paper reviews the evidence that significant amounts of fluid were generated during metamorphism and deformation of the underlying country rock as the Bushveld magma cooled and crystallized. It is here proposed that the formation of footwall diapirs led to focused flow of country fluid, resulting in the rapid influx of fluid, the formation of breccia pipes in the lower portion of the Bushveld section, and mixed with the resident magma. Irrespective of other conventional contamination events, it is shown that the introduction of 1–2% crustal fluid can significantly shift the observed Sr, Nd and stable isotopic compositions of a Main Zone magma from presumed Main Zone parent magma compositions. A numerical model of fluid generation in the footwall metamorphic aureole illustrates how country fluids develop spontaneous channels, generating diapiric activity and can be largely isolated from affecting the surrounding igneous rocks.

Finally, the results suggest that the Bushveld Complex and other large layered intrusions can be excellent analogues to understand subduction zone hydrothermal systems. Because subduction processes occur at depth and cannot be observed directly, one must rely on geophysical observations, exhumed rock (generally from shallower parts of the subduction complex), experimental methods, and numerical models understand the subduction process. The Bushveld hydrothermal system, where hot ultramafic rocks overlie dehydrating country rocks, is a natural analogue to subduction zones without the complications of faulting and a later metamorphic overprint, and can provide insights into mantle processes. Several studies analysing diapiric structures at Bushveld have drawn this connection to possible subduction zone diapirism as well (Gerya and Yuen 2003; Ireland and Penniston-Dorland 2015). Using the example of the Bushveld Complex, it is shown that metamorphic fluids can be effectively channelled by these diapirs structures and allow rapid influx of large volumes of fluid well ahead of the diapir itself for both the Bushveld and subduction systems.

2. Geology of the Bushveld Complex and associated rocks

2.1 Stratigraphy of the Bushveld Complex

The layered ultramafic to mafic rocks of the Bushveld Complex has been described as a lopolithic intrusion with a maximum thickness of about 9 km and cropping out in three main regions; the western, eastern and northern lobes. However, with an aspect ratio >30:1

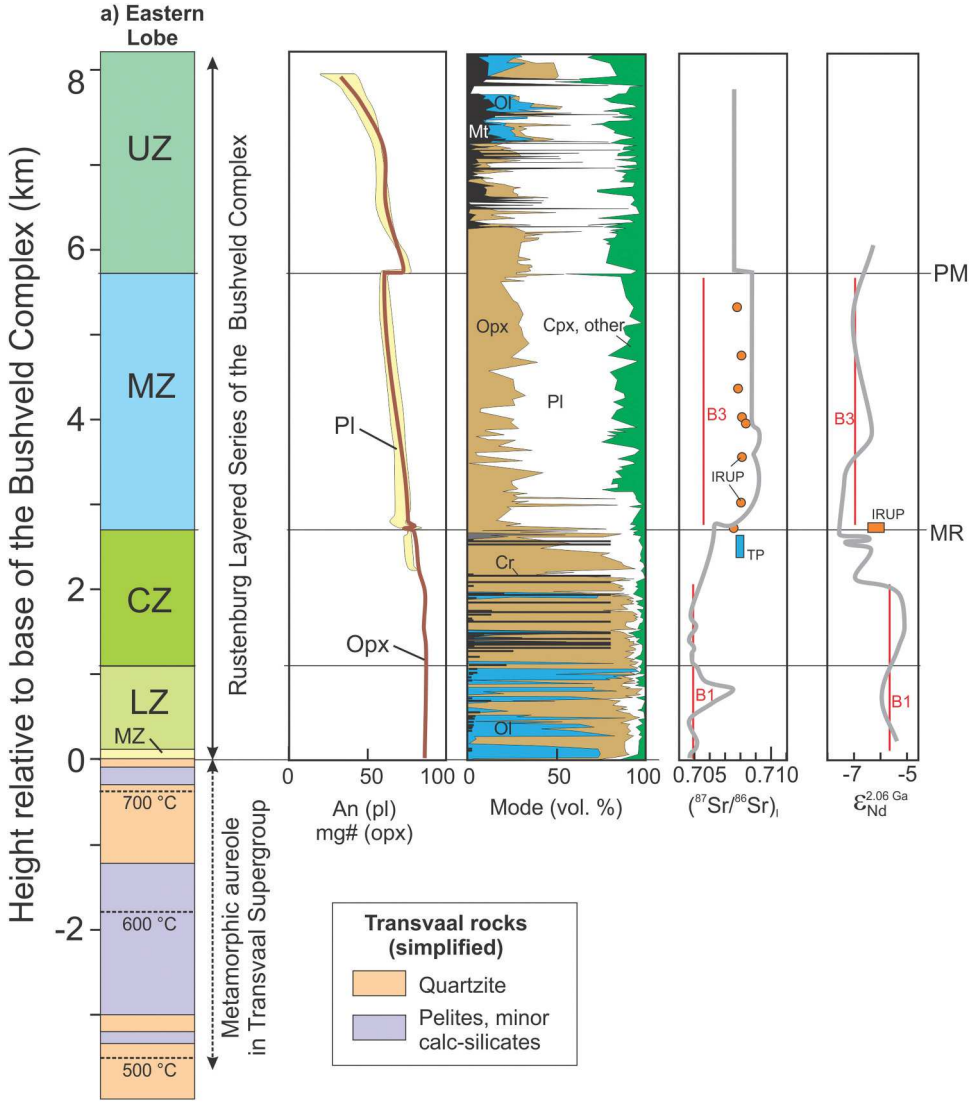

Figure 2. Main stratigraphic units, the Sr, Nd isotopic variations, and pyroxene and plagioclase compositional variation of the Bushveld Complex and its underlying metamorphic aureole. Maximum thermal isograds in the aureole are labelled. The labelled vertical grey lines in the plots of initial $^{87}Sr/^{86}Sr$ and initial ε_{Nd} isotopic trends are the isotopic compositions of the B1 and B3 sill/chilled margin rocks thought to be parental to the Lower/Lower Critical Zones and Main Zone, respectively. Orange dots indicate IRUP locations. Inset at bottom shows location map of the Bushveld Complex. Abbreviations: LZ, CZ, MZ, and UZ = Lower, Critical, Main and Upper Zones of the Bushveld Complex, respectively; MR = Merensky Reef; PM = Pyroxenite marker near top of the Main Zone; TP = Tweefontein pipe and approximate location of breccia pipe shown in ***Figure 4***; IRUP = ultramafic iron-rich pegmatoid associated with the Merensky Reef. After Kruger (1990), Maier *et al.* (2000), Cawthorn *et al.* (2000), Reid and Basson (2002), and Harris *et al.* (2003).

and locally extensive rheomorphic folding and diapirism of the floor rocks, it may be considered a variably thick sill. Palaeomagnetic evidence (e.g., Wilson *et al.* 2000; Letts *et al.* 2009) suggests that the Bushveld magma initially intruded as a horizontal sill but developed a modest dip during the emplacement of the Lebowa (Bushveld) Granite Suite soon after the formation of the Rustenburg Layered Suite. Its general geology and igneous stratigraphy have been well described and are only briefly summarized here. For a more complete discussion see Eales and Cawthorn (1996) and references therein.

The stratigraphy of the Bushveld Complex has been subdivided into five zones: a basal Marginal Zone, overlain sequentially by the Lower Zone, Critical Zone, Main Zone and finally Upper Zone (Figure 2). Evidence of a possible Basal Ultramafic Zone underlying the Marginal Zone has been found by drilling (Wilson 2015), but has not been heavily explored. The Marginal Zone is comprised of sills of locally quench-textured pyroxenites and micropyroxenites whose compositions have been interpreted as parental to the main Bushveld magmas (Sharpe 1985). The most common of these have been termed the B1 (parent to Lower Zone), B2 (Upper Critical Zone) and B3 (Main

Zone) magmas (e.g., Harmer and Sharpe 1985; Maier *et al*. 2000). The Lower Zone is approximately 800–1000 metres thick and consists primarily of layers of pyroxenite, dunite, and harzburgite with some chromite with small amounts of interstitial plagioclase, biotite, and clinopyroxene. The boundary between the Lower Zone and the Critical Zone has been defined in two ways: either a rather modest increase from about 2% to about 6% in the modal abundance of interstitial plagioclase (Cameron 1978) or by a decrease in olivine abundance (Teigler and Eales 1996). The Critical Zone is subdivided into the Upper Critical and Lower Critical Zones, with the boundary between the two occurring where plagioclase changes from an interstitial mineral to an abundant, euhedral phase. Thirteen major chromitite seams have been identified in the Critical Zone, namely, the Lower Group (LG) seams 1–7, four middle group (MG1-4) seams, and two upper group (UG) seams. The boundary between the Critical Zone and the Main Zone is usually taken to be the top of the Giant Mottled Anorthosite layer, an anorthosite with large oikocrysts of pyroxene. The Main Zone consists of a thick succession of norites and gabbronorites devoid of olivine or chromium spinel. The base of the Upper Zone is generally taken as occurring at the Pyroxenite Marker horizon (Kruger 1990) and is also marked by the appearance of euhedral magnetite (Eales and Cawthorn 1996). This zone is characterized by generally well-defined modal layering, with particularly well-developed magnetite and anorthosite layers.

These major zones are characterized by distinct variations in isotopic compositions, both radiogenic (*e.g*., Sr, Nd and Os) and stable (*e.g*. S, O and H). For instance, Nd and Sr ratios show non-monotonic and locally abrupt change moving up throughout the stratigraphic section (Figure 2). Isotopic differences can show small-scale variations between zones as well; below the Upper Zone, isotopic disequilibrium is common both within grain (core-rim) and between different minerals (*e.g*., Roelofse and Ashwal, 2012). In contrast, Sr isotopes are constant at the mineral scale and for bulk rock in the Upper Zone (*e.g*., Chutas *et al*., 2012; Schannor *et al*. 2018). Furthermore, except for a modest jump to more primitive mineral compositions at the base of the Upper Zone, stratigraphic changes in isotopic composition are not strongly mirrored by mineral compositional trends. This problem of mineral-scale isotopic disequilibrium (*e.g*., Prevec *et al*. 2005; Chutas *et al*., 2012; Yang *et al*. 2013; Roelofse and Ashwal, 2012; Roelofse *et al*., 2015) despite only modest changes in mineral composition from expected fraction trends is a long-ongoing problem. These isotopic changes are conventionally explained by variable contamination by assimilation of crustal rocks either prior to introduction into the magma chamber (*e.g*., Harmer *et al*. 1995; Maier *et al*. 2000, Harris *et al*., 2005) or by assimilation of roof rock (*e.g*., Kinnaird *et al*. 2002). Additionally, some isotope studies of Bushveld samples have been used as evidence of circulation by crustal fluids (*e.g*., Schannor *et al*. 2018).

2.2 Bushveld country rocks and the metamorphic aureole

The Bushveld magma intruded the Transvaal Supergroup of the Proterozoic Pretoria Group sedimentary rocks composed dominantly of shale, quartzite, evaporites, and lava filling the Transvaal paleobasin (to 2.5 Ga in age) (Eriksson *et al*. 1993, 1995). These rocks underwent very little deformation or thermal metamorphism before the emplacement of the Bushveld magmas. The Bushveld Complex formed a metamorphic aureole that extends at least 3.5 km (to the 500°C isotherm) beneath the base of the Bushveld sill (Figure 2). Heating of the country rock was intense enough to produce localized melting near the base of the Bushveld (Harris *et al*. 2003).

The rocks immediately below the Bushveld Complex that were thermally metamorphosed include quartzites and psammites of the Lakenvalei and Magaliesberg formations and argillaceous metasediments and minor calc-silicates of the Vermont and Silverton formations, all part of the Early Proterozoic Pretoria Group of the Transvaal Supergroup (Harris *et al*. 2003). While the country rocks immediately beneath the Bushveld Complex include the Magaliesberg quartzite which would not generate volatiles other than loss of pore fluids, the shales, carbonates and evaporates can serve as a source of volatile components in addition to H_2O.

Geologic and isotopic evidence for hydrothermal circulation related to the intrusion of the Bushveld Complex (including the Bushveld Granite) has been summarized by Gleason *et al*. (2011). Evidence includes veins in Bushveld rocks derived from Transvaal fluids (detailed more below), marginal hydrothermal ore deposits including a number of Bushveld-age Mississippi Valley-Type (MVT) mineral deposits in the Transvaal Sequence, and ~2.0 Ga palaeomagnetic overprinting of the Transvaal sediments. They suggest that a regional-scale Bushveld-age hydrothermal system circulated as far as 700 km outward from the present margins of the Bushveld.

2.3 Basement diapirs

A series of footwall upwarped dome- and trough-like structures were first mapped at the Bushveld Complex in the 1960s and 1970s. These structures locally intrude up into the Upper Zone (*e.g*., the Phepane diapir of Figure 3). The domes are important because they can channel both igneous and country fluids into the

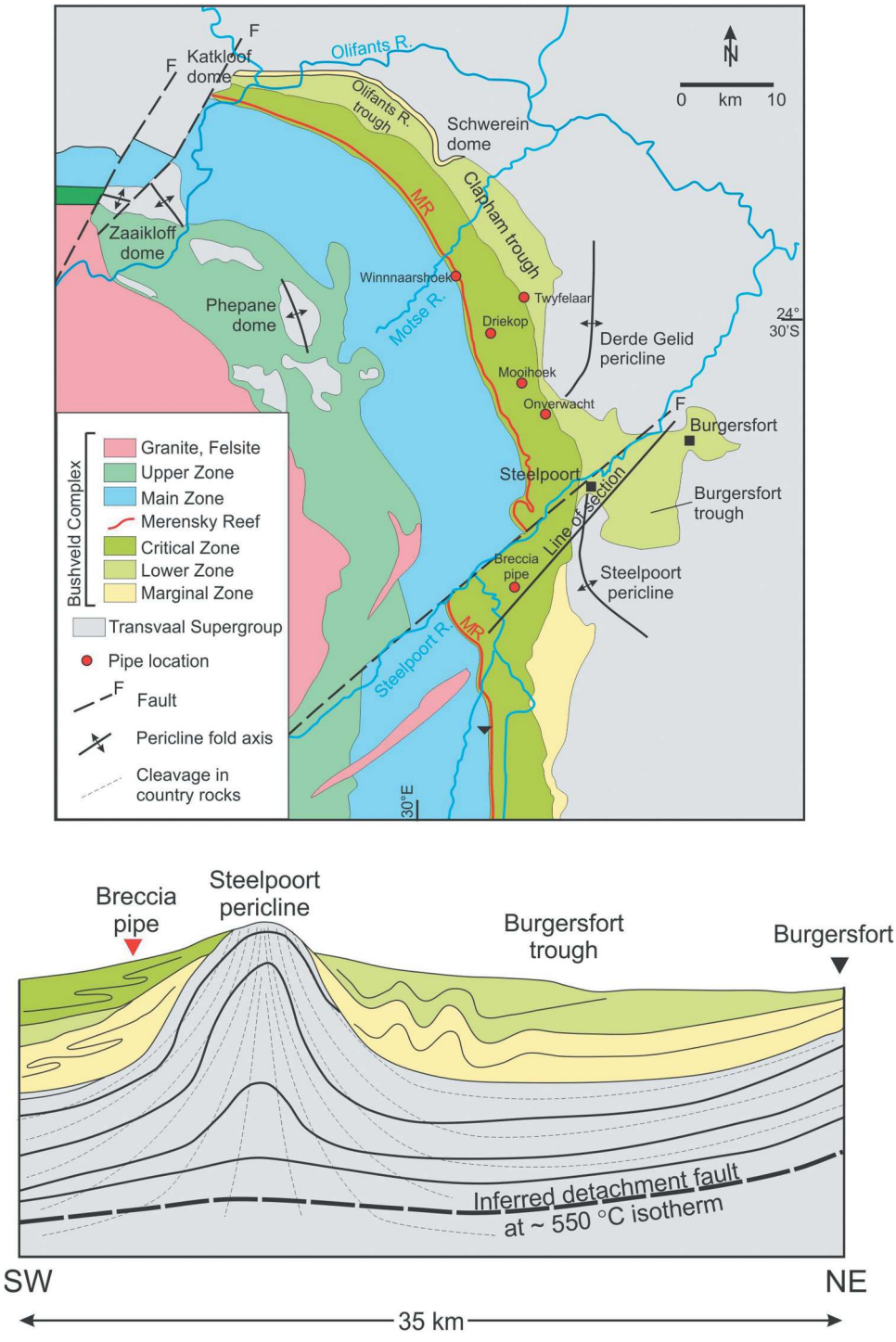

Figure 3. Detail of the geology of the part of the Eastern Bushveld Complex (top) and schematic structure cross-section across the Steelpoort pericline (bottom, no vertical scale). Location of some of the discordant pipes and the breccia pipe shown in ***Figure 4*** are also noted. The Phepane diapir is present in the northern portion of the Upper Zone. The cross-section is along the labelled 'Line of section' and illustrates the locally extensive degree of deformation in the country rock below the Bushveld as well as deformation and local thickening in the lowermost lithologic units of the Bushveld Complex. The detachment level corresponds roughly with the 550°C peak metamorphic isotherm (Uken and Watkeys 1997). Top: after Scoon and Costin (2018). Bottom: Adapted from Clarke *et al*. (2005) and published with permission from the Geological Society of South Africa.

upwarped regions. Button (1978) suggested these structures were diapiric, as the density difference between the mafic complex and the underlying sedimentary layers could easily give rise to diapirs. Since then, a number of authors have also discussed the occurrence of these features as related to syn-magmatic

deformation and diapiric upwelling (Uken and Watkeys 1997; Gerya and Yuen 2003; Clarke *et al*. 2005). Bushveld diapirism differs in some ways from typical models of diapirism. Typical diapirism involves heated, low-density floor rock material rising into the overlying cooling magma. However, the floor rock domes at Bushveld never reach the temperatures of the overlying rock (Clarke *et al*. 2005), which is why they have been termed 'cold diapirs' (Gerya and Yuen 2003; Gerya *et al*. 2004; Clarke *et al*. 2005).

Uken and Watkeys (1997) investigated the internal structure of the domes and suggested that emplacement of the northeastern Bushveld Complex was initiated by a series of finger-shaped intrusions. Folds developed between them, which provided focus for initiation of diapirism within the intrusion. Clarke *et al*. (2005) investigated deformation in the Bushveld rocks adjacent to the Steelpoort pericline. They found decreasing intensity of deformation both upwards and laterally in the intrusion and suggested country-rock diapirism as the most likely cause, as the folds would have formed due to drag and radial expansion as the diapir rose.

The petrology of the Phepane diapir was investigated by Johnson *et al*. (2004). They found evidence of spinel-cordierite symplectites replacing andalusite that they interpreted as a result of decompression, which would have occurred during the thermal peak as the diapir rose into the Bushveld rocks. Ireland and Penniston-Dorland (2015) analysed oxygen and lithium isotopes across the contact of the Phepane Dome and the Bushveld Complex host rocks itself. Their results suggest that diffusional exchange occurred for less than 5 Myr, which fits within the crystallization time predicted for the Bushveld Complex.

Numerical modelling by Gerya *et al*. (2004) utilized a Rayleigh–Taylor instability model driven by the density contrast between intrusion and sediments for subduction zones that were used by Gerya and Yuen (2003) and showed the Bushveld diapir model to be geophysically feasible. The modelled diapir growth rate of 0.8 cm/yr is consistent with that estimated by Uken and Watkeys (1997) of 0.6 cm/yr. They suggest that, while these types of diapirs have been observed only at the base of the Bushveld Complex, other layered mafic intrusions may have formed similar structures. However, Bushveld diapiric structures are only common in the thickest sections of eastern Bushveld where they intruded a sedimentary sequence that had not previously been heated. This situation is not likely to be common at other intrusions, which may limit the prevalence of similar structures elsewhere. A possible exception is seen in the Archaean-age Stillwater Complex in Montana where variations in the thickness of the Ultramafic Zone occur on about the same scale as the Bushveld structures. It has been suggested that the thicker eastern part of the Stillwater Complex formed in a subsiding basin (Raedeke and McCallum 1984); a Stillwater diapiric model would appear to be equally viable but has not yet been tested.

3. Field evidence for external fluid flow into the Bushveld Complex

3.1 Geologic evidence of external fluids

A number of features of the Bushveld Complex are suggestive of the influence external fluids may have had on the intrusion. Schiffries and Skinner (1987) and Schiffries and Rye (1990) noted the presence of high temperature (maximum temperature about 700°C) saline hydrothermal veining that cut both the intrusion and the underlying contact aureole. Schiffries and Skinner (1987) also noted the presence of fluid inclusions with highly saline, high-temperature fluid inclusions with high Cl concentrations. More recent work has shown that these are widespread throughout the Bushveld stratigraphy (Buick et al., 2001; Pronost *et al*. 2008; Roelofse and Ashwal 2008)

Associated with the diapiric structures in the Eastern Bushveld are a number of pipe-like features. One spectacular feature of the Bushveld Complex is the diatreme (breccia pipe) proximal to the Steelpoort pericline, that brings Bushveld rocks from at least the Lower Zone up into the Critical Zone (Figure 4, Ferguson and McCarthy 1970; Boorman *et al*. 2003). The breccia pipe shows features typical of rapid fluid-driven emplacement: 1) the larger blocks are concentrated on the central part of the diatreme where fluid velocities are expected to be highest; 2) elongated blocks are aligned parallel to the axis of the pipe and parallel to the inferred fluid flow direction; and 3) blocks from the deeper Lower Zone are smaller than those from the Critical Zone. Although kimberlite diatremes are an obvious analogue, it is suggested that the km-long gas blowout pipes that can occur in sedimentary basins are a more apt comparison (*e.g*., Løseth *et al*. 2011, Figure 5). The pipe illustrates that transport of large volumes of fluid can be sharply localized as it moves through the lower parts of the Bushveld Complex.

It has been previously suggested that the diatreme formed by igneous fluids generated entirely within the Bushveld mush (*e.g*., Boorman *et al*. 2003). This was based on the lack of country rock in the breccia pipe. However, the lithologies present in the diatreme that came from the deeper parts of the Bushveld stratigraphy are the smallest. Thus, it is possible that country blocks did not make it up to the level of the exposure.

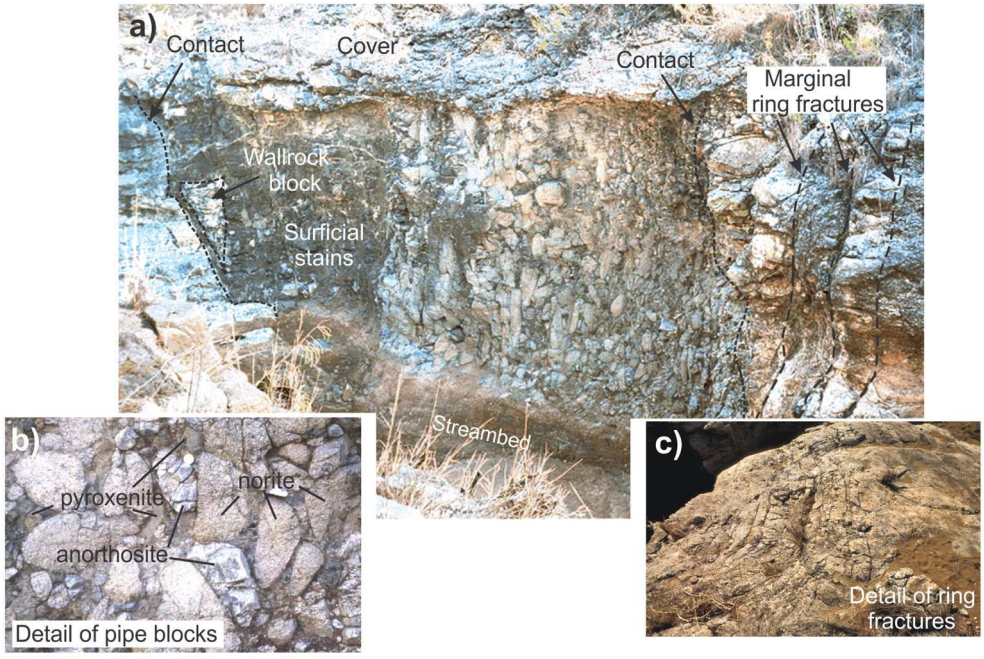

Figure 4. Diatreme (breccia pipe) from the Upper Critical Zone of the Eastern Bushveld Complex a) Overview of the pipe, interpreted to have formed by the rapid upward movement of overpressured fluid. b) Detail of the blocks from the Lower Critical Zone and the Lower Zone of the Bushveld included in the pipe. c) Ring fractures developed in the host Critical Zone rocks that surround the pipe. From Boorman *et al*. (2003), reproduced with permission.

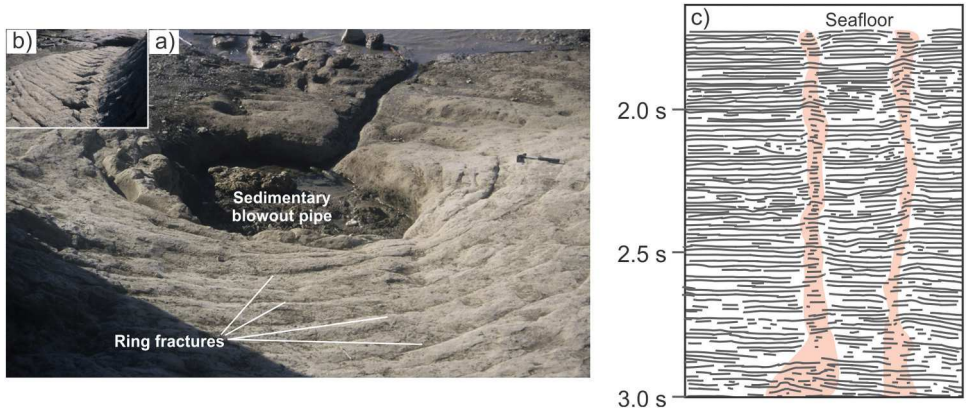

Figure 5. Sedimentary structures from by fluid overpressures as analogues for the Bushveld Breccia pipe of ***Figure 4***. a) and b) Example of pockmark at the core of a blowout pipe developed in mudrocks (from Løseth *et al*. 2011, reproduced with permission). c) Seismic sections of km-scale sedimentary blowout pipes (redrawn after Løseth *et al*. 2011).

Furthermore, brecciation might only have occurred within the crystal pile and did not reach into the footwall for reasons discussed below. While this isotopic character of the diatreme has not been studied, it does have an interstitial ultramafic component between the blocks that is similar to the iron-rich ultramafic pegmatoids (IRUP) seen elsewhere in the Bushveld Complex. Bushveld IRUP has enriched (crustal) isotopic signatures, distinct from Critical Zone rocks (Reid and Basson 2002) (the Merensky IRUP Sr and Nd isotopic compositions are shown in Figure 2).

Besides the breccia pipe, a number of discordant Mg- to Fe-rich pipes, some PGE-bearing, that occur in the lower sections of the Eastern Bushveld and have a more controversial origin (*c.f.* Scoon and Mitchell 2004 for a more detailed review). They appear to be concentrated near faults and the floor diapirs, similar as for the diatreme (Viljoen and Scoon 1985). The presence of relic chromitite layers that crosscut some of these pipes is one piece of evidence that they formed by replacement of the original lithology. While some have interpreted the

metasomatic agent to be a silicate liquid (e.g., Cawthorn *et al*. 2000; Günther *et al*. 2018) others have suggested that the iron enrichment seen in the core of the pipes are the result of metasomatic reaction involving Fe-, PGE- and Cl-rich fluids (*e.g*., Schiffries 1982).

3.2 Isotopic evidence of country fluid intrusion into the Bushveld Complex

A number of isotopic studies have suggested that very little country fluid made it into the Bushveld Complex. For example, it has been suggested that $\delta^{18}O$ in the Platreef, which occurs near the floor of the eastern Bushveld Complex, was mostly magmatic, with perhaps some interaction with calcsilicate footwall rocks resulting in lower $\delta^{18}O$ (Harris and Chaumba 2001). Harris *et al*. (2005) similarly found that elevated $\delta^{18}O$ at Bushveld was likely due to contamination at depth, in a magma 'staging' chamber. Sulphur isotope analyses have been used to suggest magmatic fluid backflow into the country rock, rather than from the country rock into the intrusion, occurred at Bushveld (Penniston-Dorland *et al*. 2008). Ireland and Penniston-Dorland (2015) measured lithium isotope variations at the base of the Bushveld Complex. They find deeper penetration of Li country-rock signatures (~60 m) compared to oxygen signatures (~4 m) but suggest that this is due to the higher diffusivity of Li rather than country fluid contamination. Chlorine isotopes suggest that Bushveld Cl is isotopically distinct from the country rocks (Willmore *et al*., 2002).

In contrast with this evidence are isotopic signatures consistent with a deeper penetration of country fluids into the Bushveld Complex. For example, Schiffries and Rye (1990) noted that although the $\delta^{18}O$ of the late-stage veins that cut the Bushveld was controlled by isotopic exchange with the Bushveld intrusive rocks, the δ^{13} C and δD was inherited from the Transvaal rocks. Buick *et al*. (2000) had a similar interpretation. In addition, Mathez and Waight (2003) noted Pb isotopic disequilibrium between plagioclase and sulphide of the Upper Critical Zone. They suggested that some of the Pb originated from the isotopically distinct country rocks and was introduced at temperatures at which the composition of sulphide but not plagioclase could be modified. Chutas *et al*. (2012) suggested much of that same thing to explain Sr disequilibrium between plagioclase and orthopyroxene of the Critical Zone. They proposed that orthopyroxene was more likely to be affected by an infiltrating metasomatic agent as it underwent exsolution on cooling. Magalhães *et al*. (2018) found evidence of laterally homogeneous but stratigraphically variable crustal S signatures throughout the Bushveld Complex. The variations they observed were correlated to variations in $^{87}Sr/^{86}Sr_i$ and ε_{Nd}, although not systematically, which suggests the involvement of multiple contaminants. Although Magalhães *et al*. (2018) do not consider fluids due to lack of textural evidence, variations in S isotopes corresponding to Sr and Nd variations may indicate that these variations are also fluid-related. More recently, Schannor *et al*. (2018) suggested that higher initial $^{87}Sr/^{86}Sr$ of plagioclase in the UG2 chromitite and the footwall pyroxenite reflects infiltration of fluid derived from dehydrating country rocks beneath the Bushveld Complex. Zeh *et al*. (2020) analysed Hf isotopes in zircon grains and found overlapping ε_{Hf} values in the RLS and the contact aureole which they suggested could have been achieved by aqueous fluid infiltration from the contact aureole.

In short, while a number of studies have examined variations in isotopic ratios throughout the Bushveld Complex, many have been limited in the scope they have considered. The majority examine isotopic alteration of the solid assemblage; in some cases, alterations that occurred during flux melting. While a number of studies note that isotopic variations throughout the Bushveld are likely related to country-rock contamination, most do not look seriously at the possibility that fluids contaminated the magma. As this study will demonstrate, fluids have great potential to explain a large number of observed isotopic variations. In addition, this fluid ingress may have been distinctly channelled, as seen in the breccia pipes and other features; numerical models presented here highlight this fluid channelling.

4. Footwall dehydration and fluid overpressure

The breccia pipe noted above points to the development of considerable fluid volumes and overpressure to drive pipe formation. Typical crustal rocks can lose 3–6% of their mass to dehydration during metamorphism (Connolly 2010). This is equivalent to a body of water roughly 90–180 metres deep for each kilometre of rock dehydrated, and it is the release of this water that likely weakens the host rock and promotes diapir formation. Furthermore, the intrusion of the Bushveld magmas into previously unmetamorphosed sediments is rather unique; many other (large) intrusions are hosted by high grade metamorphic or granitic rocks. A comparison between the Bushveld and the Stillwater Complex in south-central Montana illustrates this difference. Comparing the H_2O contents of pelite as a function of temperature (Figure 6), the biotite schist that hosts the Stillwater Complex would have but a fraction of the H_2O content of a lower temperature shale or slate intruded by the Bushveld magma.

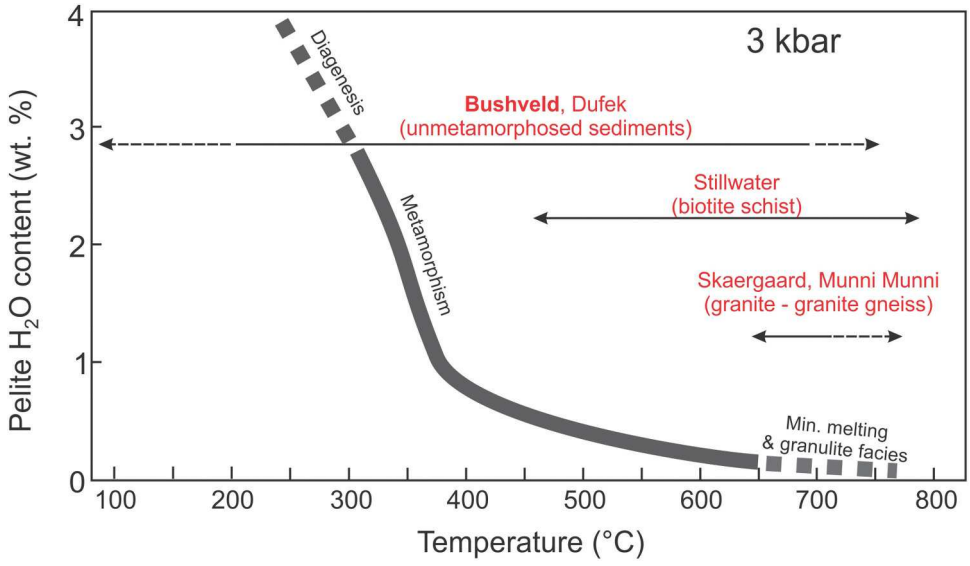

Figure 6. Progressive loss of H_2O in a typical pelite undergoing prograde metamorphism as a function of temperature at 3 kbar total pressure (after Connolly 2010). Calculation assumes pure H_2O, and reactions involving CO_2 are ignored. Also noted are the approximate metamorphic temperatures seen in host rock prior to emplacement of some selected intrusions as discussed in the text.

Furthermore, crystallization and thermal modelling of the Bushveld Complex show that a considerable thickness of crystal pile can accumulate prior to reaching the thermal maximum in the basement rock (e.g. Cawthorn and Webb 2013). Near the base of the Layered series, temperatures of the igneous rocks and immediately underlying country rocks are similar and fluids moving from a pyroxene hornfels into a Bushveld pyroxenite can be in roughly chemical equilibrium. The influx of fluid may not be clearly evident in any obvious mineral reactions in the rock, in what one might term *cryptic flow*.

A first-order model for the understanding of how breccia pipes can develop during dehydration of the underlying country rock is shown in Figure 7 (after Connolly 2010; Connolly and Podladchikov 2013). In this figure, fluid is generated at the base of the sill by dehydration of the country rock; fluid generated within the intrusion is ignored. If the rocks are also undergoing compaction, then the lithostatic load pressing on the fluid at the base of the fluid generation zone will be transferred upwards by the fluid. Compaction at the base squeezes fluid upwards to the upper portion, producing a high porosity region where it is accommodated by dilational deformation. This process has the effect of propagating the reaction-generated porosity upwards and into the lower part of the sill. As long as fluid transport can keep up with the developing fracture network and if fluid flow is rapid enough, the result is brecciation and explosive injection of country fluid into the magma chamber. However, as shown in the numerical modelling below, the high porosity region can detach from the source when the compaction rate at the base becomes comparable to the fluid production rate, giving rise to solitary waves that propagate upwards independently of its source (Connolly and Podladchikov 2013).

5. Isotopic consequences of fluid injection into the Bushveld magma chamber

The possibility of country fluid contamination of the Bushveld magma adds an additional degree of freedom to Bushveld isotope geochemistry. Currently, isotopic variation between zones has made it challenging to fully understand the origin and development of the Bushveld Complex. Conventional contamination models have often relied heavily on high amounts of crustal contamination (30–40%, Maier *et al*. 2000; Harris *et al*., 2005) and/or magma mixing to explain isotope compositional variations in the Bushveld. For example, Maier *et al*. (2000) noted the Lower and Lower Critical Zone samples have similar Sr and Nd isotopic compositions compared to their assumed parental magmas, the B1 sill and chilled margin. The B1 and the Lower and Lower Critical Zones also have similar incompatible trace-element ratios (*e.g*., Sm/La and Th/La). The Main Zone also has similar incompatible element ratios and Nd isotopes to its assumed parental magma, the B3 sill/chilled margin. However, the Main Zone rocks have distinctly more radiogenic Sr (0.708 vs. 0.7055) than

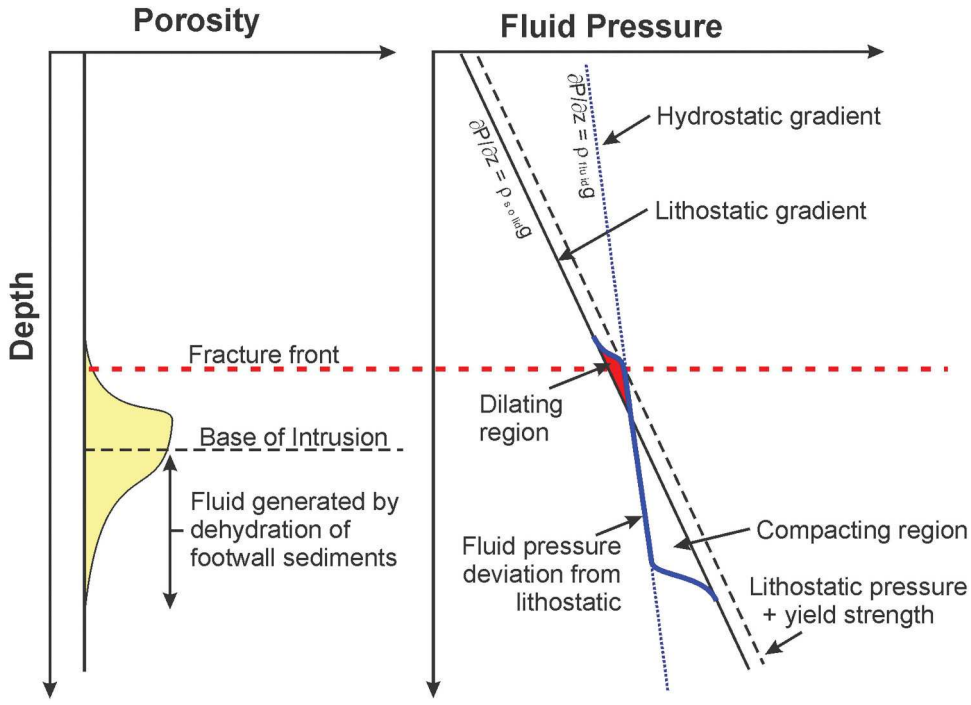

Figure 7. Schematic example of the generation of overpressured fluid by degassing and compaction of the lower portions of the Bushveld Complex and footwall sedimentary rocks (after Connolly 2010; Connolly and Podladchikov 2013). The absence of footwall rocks in the diatreme suggests the overpressured fracture and brecciation began within the Lower Zone of the Bushveld Complex. Because the absolute pressure is depth-dependent, the overpressure is scaled relative to the difference between a lithostatic gradient for the rock and a hydrostatic gradient for a connected pore fluid. Compaction occurs where the lithostatic pressure exceeds the hydrostatic pressure, and dilation where the hydrostatic pressure exceeds the lithostatic pressure. The net effect is the upward movement of a high porosity (fluid-rich) region into the sill. See text for additional discussion.

does the B3 sill/chilled margin sample. These isotopic variations are illustrated in Figure 2. To explain these variations, conventional models of crustal contamination or magma mixing require some contortions, which can be relaxed under an assumption of country fluid contamination.

5.1 Mixing model assumptions

To illustrate the effect of vapour addition to the Main Zone magma, a number of simple mixing models are shown. A wide variety of isotopic studies have been conducted at Bushveld; some have been discussed above. These mixing calculations include Sr, Nd, O, H, S and Pb. For these calculations, the complication of isotopic disequilibrium, noted previously, is ignored. The composition of a fluid derived from Bushveld country rocks is not well-constrained. Thus, fluid concentrations of the isotopes in question are based on fluid inclusion studies from other locations, such as Sudbury. Parental magma compositions are limited by available data. Where possible, isotopic signatures of Marginal Zone rocks, particularly B3 samples generally considered to represent Main Zone parental magmas, are used in the calculation. Although these Marginal Zone samples may already be contaminated by assimilation of Transvaal materials or deeper crustal rocks, the isotopic and trace-element ratio similarity between B1 and much of the Lower and Critical Zones suggests that the B3 is the best candidate for the original Main Zone magma. Furthermore, fluid contamination need not be the only source of crustal contamination in the intrusion; this work means only to highlight that it can contribute to contamination of the Bushveld. For isotope systems where Marginal Zone data are not available (S, Hf), parental magmas are assumed to be mantle-derived; assumptions for these isotopic systems are discussed in more detail below. All mixing models are shown in Figures 8 and 9. Details of the mixing models are as follows:

A Sr-Nd mixing calculation (Figure 8) is based on a parental magma of the B3 isotopic composition (Maier *et al*. 2000) and a poorly constrained fluid. The Sr content of the vapour (4400 ppm) is that reported for average Sudbury brine inclusions (Hanley *et al*. 2005) and is assumed to have an initial Sr isotopic composition of a Bushveld footwall schist (Sr_i = 0.722; Maier *et al*. 2000). For Nd, fluid concentrations of 10, 20 and 30 ppm are shown; 10 ppm is a high value also from Sudbury fluid inclusions (again, from Hanley *et* al). A typical upper

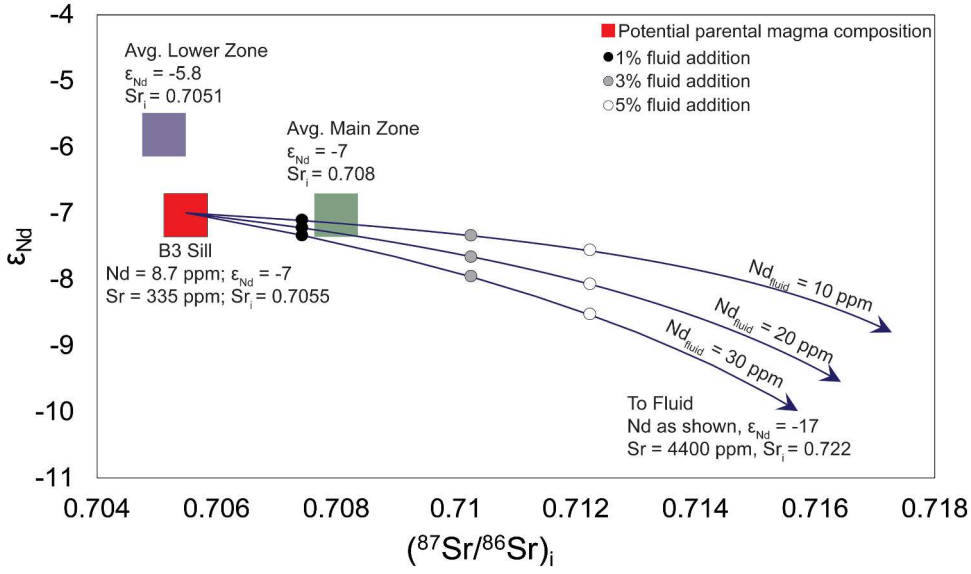

Figure 8. A fluid-magma Sr-Nd isotope mixing model for the Main Zone rocks (relative to the presumed initial Main Zone magma, denoted 'B3') of the Bushveld Complex. Endmember mixing components are as listed, and the points on the mixing line indicate 1% (black), 3% (grey), and 5% (white) weight fraction of vapour in the mixed composition. The three mixing lines are for different Nd concentrations in the endmember vapour, as labelled. The compositions of the B3 magma, the Lower Zone, and the Main Zone are shown by the coloured boxes labelled 'B3 Sill', 'Avg. Lower Zone', and 'Avg. Main Zone', respectively.

crustal ε_{Nd} of −17 is used for Nd (also from Maier *et al.*). Nd and Sr data for the Bushveld Complex Main Zone are taken from Maier *et al*. (2000) as well.

In mixing $\delta^{18}O$ and δD, the parental magma was assumed to approximate the lowest $\delta^{18}O$ and δD of Marginal Zone samples. Also shown on this mixing diagram are the isotopic compositions of several potential magmatic source regions for the Bushveld, including MORB ($\delta^{18}O$ = 5.7‰; Ito *et al*. 1983; Eiler 2001, δD = −80‰; Kyser and O'Neil 1984), boninite ($\delta^{18}O$ = 6.5‰; Kyser *et al*., 1986, δD = −55‰; Dobson and O'Neil 1987), and komatiite ($\delta^{18}O$ = 5.2‰, Lahaye and Arndt 1996; δD = −140‰, Stone *et al*. 2003). The 'true' parental magma(s) of the Bushveld Complex are a matter of some debate (*e.g*., Barnes 1989). We suggest the Marginal Zone values of ~6.8‰ used as parental compositions have experienced assimilation of dry crustal material that substantially altered $\delta^{18}O$ but not δD. Concentrations of O are calculated from the total O contents of average B3 samples (Sharpe 1981). H contents of a typical mantle magma are calculated at approximately 300 ppm, based on H_2O contents of a typical MORB (0.17–0.51 wt. %, Sobolev and Chaussidon 1996). Country fluid isotopic compositions were estimated based on country-rock measurements as well as analyses of fluid inclusions. $\delta^{18}O$ in the metamorphosed hornfels of the Transvaal Supergroup range from 9‰ to 15‰ (Schiffries and Rye 1989); fluid fractionation has the potential to raise this by a few per mille (Shieh and Taylor 1969), bringing $\delta^{18}O$ to 20‰. δD values from a number of sources suggest a wide range of possible values for country-rock hydrogen isotopes. Schiffries and Rye (1990) identified a δD range of −71‰ to −29 from fluid inclusions. The hydrogen concentration in a dehydrated fluid is poorly constrained; we use 11% H concentration as a maximum estimate. Also shown are $\delta^{18}O$ (Schiffries and Rye 1989; Schiffries and Rye 1990; Harris *et al*., 2005) and δD (Mathez *et al*., 1994; Willmore *et al*., 2002; Harris *et al*., 2005) from the Bushveld Complex itself.

Several authors have noted distinct Pb isotopic disequilibrium between minerals in Bushveld samples (*e.g*., Mathez and Waight 2003; Mathez and Kent 2007; Chutas *et al*., 2012). This has been suggested to be the result of alterations to Pb isotopic composition around the time of crystallization, but after certain minerals (such as plagioclase) had closed to isotopic alteration. The low U contents of relevant minerals suggest no radiogenic ingrowth to impact initial Pb isotopic compositions, although the mobility of U means this is not a guarantee (Harmer *et al*. 1995; Mathez and Waight 2003); Bushveld Pb isotopic ratios are assumed to represent true initial ratios. Pb typically shows evidence of substantial alteration during cooling, while plagioclase shows less evidence of this due to an earlier closure. Pb contents in an initial Bushveld parental magma would be low; because Pb is mobile, a fluid can be highly Pb-enriched relative to the parental magma. B3 compositions suggest a parental magma for the Bushveld may have contained roughly 1.5 ppm Pb (Harmer *et al*. 1995). Fluid inclusions from Sudbury have Pb concentrations of

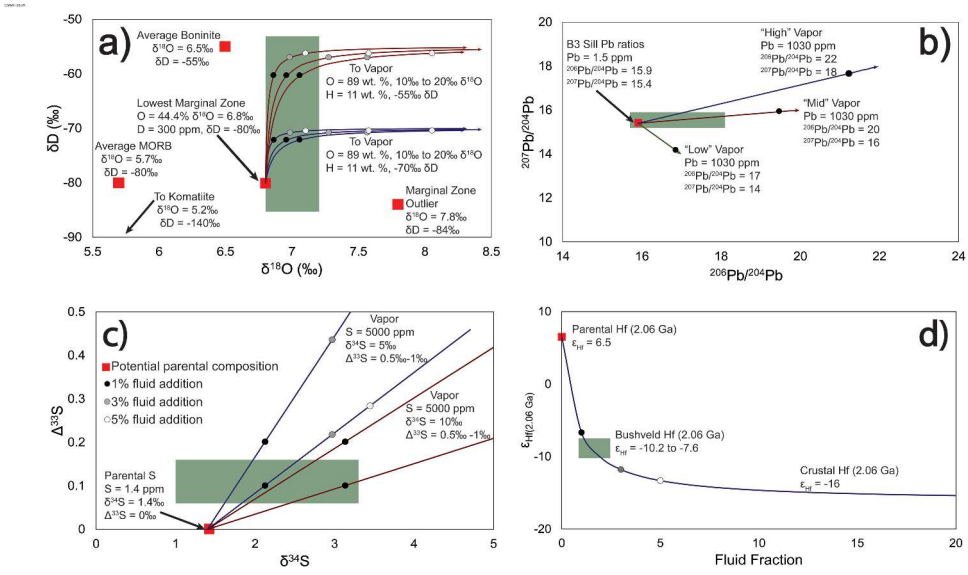

Figure 9. Examples of fluid-magma mixing models. In all mixing models, the red boxes highlight potential parental magma compositions. Black, grey, and white points on mixing curves indicate 1%, 3%, and 5% fluid addition, respectively. a) A fluid-magma mixing model explaining alteration in $\delta^{18}O$ and δD compositions throughout the Bushveld Complex relative to a parental magma resembling the lowest Marginal Zone sample. Endmember mixing components are listed. The labelled lines show differing fluid $\delta^{18}O$ compositions. Due to relative lack of variation in isotopic ranges for $\delta^{18}O$ and δD throughout the Bushveld Complex, the Bushveld as a whole is displayed as one region on the plot. b) A fluid-magma mixing model for $^{207}Pb/^{204}Pb$ and $^{206}Pb/^{204}Pb$ variation in the Bushveld Complex. Due to the high Pb contents of the fluid relative to the magma, mixing is strongly dominated by potential country-rock fluid Pb sources. Each mixing lines indicates a different potential source. c) A fluid-magma mixing model for S isotopes, showcasing both $\delta^{34}S$ and $\Delta^{33}S$ variation. Blue lines use vapour $\delta^{34}S$ of 5‰ while red lines use vapour $\delta^{34}S$ of 10‰. $\Delta^{33}S$ for the vapour is either 0.5‰ (lower mixing line) or 1.0‰ (upper mixing line). d) A fluid-magma mixing model for ε_{Hf} variation, plotted against fluid fraction. Green line at $\varepsilon_{Hf} = -8.6$ shows Bushveld composition at the time of emplacement.

1.03 wt. % (10,300 ppm); reducing this by a factor of 10 in the event of low Pb concentrations in Transvaal sediments brings this value to 1,030 ppm for the fluid. B3 magmas contain $^{206}Pb/^{204}Pb$ of 16 and $^{207}Pb/^{204}Pb$ of 15.4 (Harmer *et al*. 1995). The question of the Pb isotopic ratios in Transvaal sediments is complicated by the issue of Pb and U mobility as well as radiogenic ingrowth. While Pb isotopic ratios have been measured in a number of Transvaal sedimentary groups (dolomites, Jahn *et al*. 1990; Campbellrand Supergroup, Sumner and Bowring 1996; Black Reef pyrites; Barton and Hallbauer 1996), radiogenic ingrowth and subsequent Pb loss have made reliable calculation of initial Pb compositions challenging. For this reason, the mixing plot for Pb shows mixing for several possible initial isotopic compositions, based in part on standard upper crust Pb ratios and in part on discussions of measured Pb ratios and calculated μvalues in Transvaal sediments. Because the Pb_{fluid}/Pb_{magma} ratio would have been high, the unconstrained initial Pb ratios of the sediments are the largest source of error in this calculation. However, Figure 9b shows that alteration of magmatic Pb isotope ratios can occur with little fluid addition.

S isotopes have two common isotopic signatures that are analysed; $\delta^{34}S$ tracks mass-dependent fractionation while $\Delta^{33}S$ is a measure of mass-independent fraction caused by Archaean atmospheric conditions (Farquhar and Wing 2003). Analyses of both S isotopic measurements have been made throughout different limbs of the Bushveld Complex (*e.g*., Sharman-Harris *et al*. 2005; Penniston-Dorland *et al*., 2012). Multiple sulphur isotope studies of the eastern and western limbs of the Bushveld found $\Delta^{33}S$ = 0.06–0.16‰ and $\delta^{34}S$ = 1.0–3.6‰ (Penniston-Dorland *et al*., 2012; Magalhães *et al*., 2018). Two samples measured by Magalhães *et al*. (2018) were found to have much lower $\delta^{34}S$ of 0.58‰ and −1.19‰. These samples were outliers compared most other samples and may reflect less contamination or assimilation of country-rock sulphur from a different source (*e.g*., Transvaal pyrite with negative $\delta^{34}S$; Strauss and Beukes 1996). Mantle $\delta^{34}S$ and $\Delta^{33}S$ are well established at 0 ± 2‰ and 0 ± 0.03‰, respectively (*e.g*., Ripley *et al*. 1999; Farquhar *et al*. 2002). Labidi *et al*. (2012), using a different extraction technique, found a more narrow range of −1.8‰ to 0.02‰ for $\delta^{34}S$ originating from the DM (depleted mantle) reservoir; modelling isotope

mixing with their average DM $\delta^{34}S$ of 0.91‰ resulted in mixing lines shifted somewhat towards lighter $\delta^{34}S$ values and carrying most mixing lines out of the range of Bushveld S isotope values. However, Sharman-Harris *et al*. (2005) suggest a $\delta^{34}S$ value of 1.4‰ as the original parental composition based on sulphide inclusions from beneath the craton; this is the value used in S isotope modelling shown in Figure 9c. 0‰ is used as the $\Delta^{33}S$ parental value for S isotope mixing calculations. Unaltered mantle is thought to contain ~200 ppm S (Nielson *et al*. 2014). S contents of a hydrothermal vapour or fluid phase are poorly quantified due to the difficulty in detecting sulphur-bearing species in fluid inclusions (Pokrovski *et al*. 2005). A fluid concentration value of 5000 ppm is chosen for S as a conservative, rough estimate of S alone. Transvaal sediments exhibit a wide range of $\delta^{34}S$ values; Penniston-Dorland *et al*. (2012) use −0.4‰ to 5‰ for $\Delta^{33}S$ and Strauss and Beukes (1996) find a $\delta^{34}S$ range of ~3-20‰. Because high values of S isotopes are not common, mixing calculations for S isotopes utilize mid- to low-range values of $\delta^{34}S$ = 10‰ and 5‰ and $\Delta^{33}S$ = 1‰ and 0.5‰, respectively.

The Bushveld Complex has observed Hf isotopic compositions that differ substantially from those that would be found in a theoretical komatiite parental magma. Zirackparvar *et al*. (2014), VanTongeren *et al*. (2016), and Zeh *et al*. (2019) have explored Hf isotopes in zircons at Bushveld and associated sediments. Zirakparvar *et al*. and VanTongeren *et al*. found relatively uniform Bushveld $\varepsilon_{Hf\ (2.06\ Ga)}$, values of −8.6 (±2.6, Zirakparvar *et al*.; ±1.2, VanTongeren *et al*.) for 2.06 Ga (Bushveld emplacement). Zeh *et al*. (2019) found a range in $\varepsilon_{Hf\ (2.06\ Ga)}$in Bushveld Complex mafic floor rocks of −10.2 to −7.6. In lieu of more specific Hf constraints on a parental magma for Bushveld, a komatiite parent is assumed (Barnes 1989; Zirackparvar *et al*. 2014). A komatiite magma would have $\varepsilon_{Hf\ (2.06\ Ga)}$ of +6.5 (Zirackparvar *et al*. 2014). Komatiite magmas have Hf concentrations of ~0.715 ppm (again from Zirackparvar *et al*. 2014). Transvaal sediments exhibit a range in $\varepsilon_{Hf\ (2.06\ Ga)}$ values; the Hf mixing model here utilizes $\varepsilon_{Hf\ (2.06\ Ga)} = -16$ (Zeh *et al*., 2019). Fluid incorporation of Hf is a complicating factor. As a HFSE, Hf typically experiences low mobility in aqueous fluids, instead migrating during partial melting (*e.g*., Barry *et al*. 2006). However, there is evidence that fluid Hf enrichment of a few hundred ppm can occur under certain circumstances (*e.g*., Zeh *et al*. 2010; Zeh and Gerdes 2014). For this reason, the Hf mixing model uses a fluid Hf concentration of 200 ppm.

5.2 Discussion of model results

Taken together, these mixing calculations demonstrate that the addition of roughly 1 wt. % of a country fluid can pull the B3 composition towards the more typical Main Zone isotopic composition. Assuming that the 3.5 km thick Bushveld aureole (to 500°C isotherm) generated 3–6 wt.% H_2O, the addition of 1–2 wt.% vapour to the 2–3 km enriched section of the Main Zone would require about a third to half of vapour generated from footwall dehydration was injected into the Main Zone. ***Table 1*** provides a summary of the impact of this amount of fluid on the various isotopic systems for which there are sufficient data at the Bushveld Complex. Some isotopes are more strongly impacted than others. For example, δD and Sr are relatively sensitive to the addition of vapour, while $\delta^{18}O$ and Nd are less sensitive. This is likely due to relative concentrations of these elements between the vapour and the parental magma; higher concentrations of an element in the parental magma leads to the vapour having a less noticeable comparative impact. Table 1 includes the expected isotopic shifts of several isotopic systems not shown in Figure 9. These

Table 1. Effect of 1% fluid addition in modification of B1 isotopic composition. The effect on the B3 magma is similar.

	Parental Magma		Sediment-Derived Fluid		
System	Conc. (ppm)	Int. Value (2.06 Ga)	Conc. (ppm)	Int. Value (2.06 Ga)	Effect of 1% fluid addition
Radiogenic Isotopes					
$^{87}Sr/^{86}Sr$	158	0.705	4,400	0.722	+0.002
$^{143}Nd/^{142}Nd$	20	$\varepsilon_{Nd} = -5.8$	20	$\varepsilon_{Nd} = -17$	$\Delta\varepsilon_{Nd} = -0.2$
$^{176}Hf/^{177}Hf$	0.715	$\varepsilon_{Hf} = 6.5$	200	$\varepsilon_{Hf} = -16$	$\Delta\varepsilon_{Hf} = -12$
$^{206}Pb/^{204}Pb$	1.5	15.9	1030	17 to 22	+1 to +5
$^{207}Pb/^{204}Pb$	1.5	15.4	1030	14 to 18	−1 to +2
Stable Isotopes					
$^{18}O/^{16}O$	440,000	$\delta^{18}O = 5.7$‰	890,000	$\delta^{18}O = 10$ to 20‰	+0.2‰
D/H	600	δD = −80‰	110,000	δD = −70 to −50‰	+10 to 20‰
$^{37}Cl/^{35}Cl$	500	$\delta^{37}Cl = 3.0$‰	50,000	$\delta^{37}Cl = 1.0$‰	−1‰
$^{13}C/^{12}C$	200	$\delta^{13}C = -5.0$‰	10,000	$\delta^{13}C = -2.5$‰	+1‰
$^{34}S/^{32}S$	200	$\delta^{34}S = 1.4$‰	5000	$\delta^{34}S = 5$‰ to 10‰	+1.7‰
$\Delta^{33}S$	200	$\Delta^{33}S = 0$‰	5000	$\Delta^{33}S = 0.5$‰ to 1‰	+0.1 to 0.2‰
Li	1.5	$\delta^{7}Li = 3$‰	200	$\delta^{7}Li = 20$‰	+9‰

include chlorine, carbon, and lithium. Few studies have been conducted on these isotopic systems at Bushveld (Cl, Willmore *et al*., 2002; C, Pronost *et al*. 2008; Li, Ireland and Penniston-Dorland 2015). However, these isotopic ratios can also experience substantial alteration from a small amount of fluid; further investigations into these systems are required to better identify large-scale alterations from expected magmatic values.

Theoretically, the fluid could also be contaminated by the Lower Zone rocks it passes through. However, the fluid is relatively insensitive to this potential contaminate. This is again due to relative concentrations; typical Lower Zone concentration of Sr and Nd is about 20–40 ppm and 1–2 ppm, respectively (Maier *et al*. 2000). These values are largely controlled by the amount of trapped liquid. While fluid contamination by Lower Zone rocks is possible and would tend to pull the fluid towards a higher ε_{Nd}, this would require equilibration with a substantial mass of Bushveld rock.

In comparison to the results of other contamination models (*e.g*., Maier *et al*. 2000; Harris *et al*., 2005; Penniston-Dorland *et al*., 2012; Zirackparvar *et al*. 2014), our results demonstrate a need for substantially less contamination. Maier *et al*. (2000), analysing Nd and Sr isotopes, found that pulling Bushveld parental magmas to the modern measured isotope signatures required that as much as 40 to 50 wt. % of the Main Zone be crustal in origin. Harris *et al*. (2005) suggested that mixing $\delta^{18}O$ between crust and parental magma would require 38% contamination. Similarly, Zirackparvar *et al*. (2014) suggested that producing the observed $^{176}Hf/^{177}Hf$ shifts would require incorporation of 80% Hf from the crust. Because a fluid will preferentially incorporate and become enriched in some elements, a crustal fluid source for this same contamination requires much less addition of the contaminant. As shown in Table 1 and Figures 8 and 9, 1–2 wt. % of a fluid (which can realistically be generated by Bushveld emplacement) can be responsible for observed shifts in isotopic ratio. Because incorporation of 30% or more crustal material would have additional resulting complications, we suggest that Main Zone equilibration with a smaller amount of fluid isreasonable.

6. Modelling fluid migration associated with the footwall metamorphic aureole

6.1 A quantitative model of fluid flow during dehydration of the floor rocks

To illustrate the pattern of metamorphic fluid flow that might have arisen beneath the Bushveld Complex, a 2-dimensional thermomechanical finite-difference model was used to simulate metamorphic devolatilization and compaction-driven fluid expulsion beneath the sill (Connolly and Podladchikov 2007; Connolly 2010, Figure 10). The spatial domain is a 1 km wide section that extends from the surface to 20 km depth and is resolved with a nodal spacing of 20 m. The sill is 8 km thick and emplaced instantaneously at 6 km depth in crustal rocks with a geothermal gradient of 30 K/km. Only part of this spatial domain is shown in Figure 10, which is centred on the lower contact of the sill. The initial temperature of the sill is its assumed liquidus (1500 K). The solidus temperature is taken to be 1200 K, and the latent heat of crystallization (0.3 MJ/kg) is released as a linear function of temperature. For simplicity, a single muscovite dehydration reaction is considered with kinetic and thermodynamic parameters after Connolly (1997a). The equilibrium dehydration temperature immediately below the sill is ~850 K (and increases with depth by ~36 K/km) and is thus roughly 370 K below the initial temperature of the footwall rock. A 200 m thick inert layer is included at the top of the country rock to mimic the Magaliesberg quartzite and to improve numerical stability.

Fluid expulsion is assumed to be initially controlled by the rate at which viscous compaction collapses the fluid-filled porosity generated by the dehydration process. Once a wave has nucleated its properties are independent of what happens in the source, that rate of wave propagation depends on rock and fluid viscosities and densities. Furthermore, it is assumed that embrittlement caused by the generation of high fluid pressures by dehydration and/or compaction can be characterized by a reduced effective viscosity. The governing equations are for the flow of a low viscosity fluid through a viscous solid with finite porosity. In applying this model to the lower portion of the Bushveld Sill, the assumption is made that the crystal mush can be approximated as a porous low viscosity solid. In reality, the true three-phase system (silicate-liquid, water-rich fluid, and solid) is likely to be substantially more complex. In particular, water released by dehydration of the footwall rocks will both dissolve in the silicate liquid and lower the solidus of the silicate liquid. In view of these simplifications, the viscous rheology of both the country rocks and crystal mush is taken to follow a single power-law constitutive relation based on the properties of quartz (Schiffries and Rye 1990), likewise the permeability (k) of both mush and country rock is characterized by a single power law relation with porosity (ϕ). Both the country rocks and sill are assigned a small initial porosity randomly distributed in the range 0.05–0.15%.

Previous work (Connolly and Podladchikov 2007) has shown that fluid flow in this scenario is channelled into

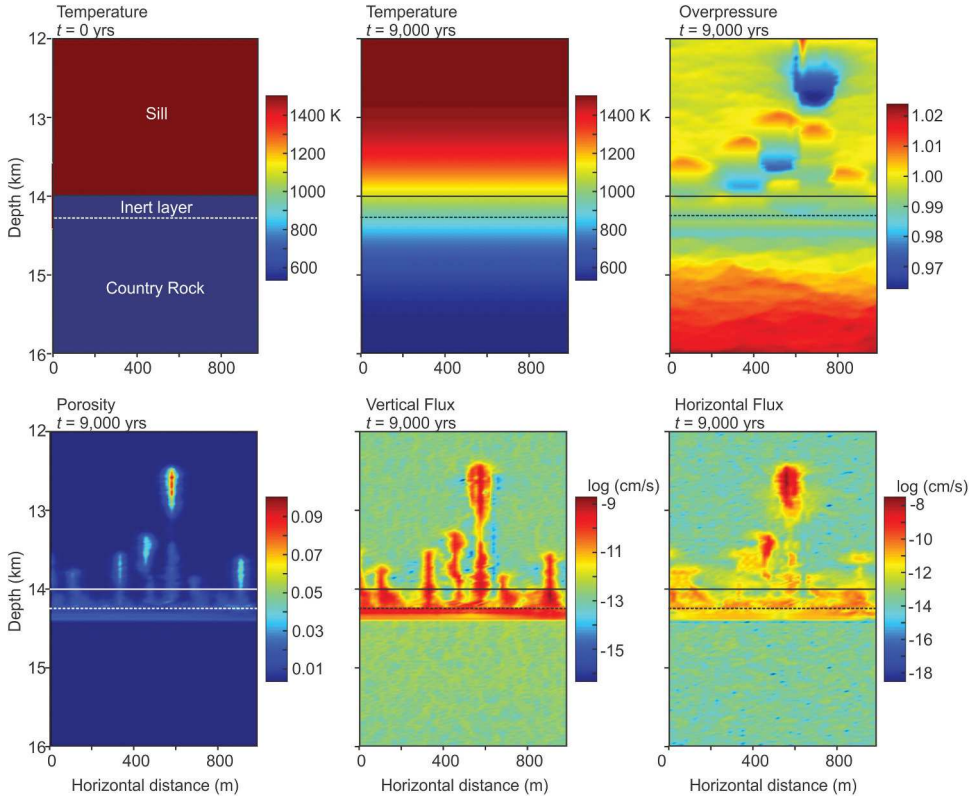

Figure 10. Numerical model of footwall dehydration and volatile plume formation. Upper left shows the initial condition of a hot sill intruded into sediments with a geothermal gradient ranging from 573 K at the bottom to 1473 K at the top at $t = 0.0$. A 200 m thick inert layer is included at the top of the country rock to mimic the Magaliesberg quartzite and to improve numerical stability. All other figures show the system after $t = 9{,}000$ years. Upper centre and upper left shows the thermal profile and overpressure. The bottom three figures show the porosity, vertical, and horizontal flux, respectively. The steep front of vapour flux at the base of the metamorphic aureole mimics the steep fluid generation front (not shown). A video of the numerical model is available as part of the on-line supplemental material. See text for additional discussion.

pipe-like structures with a characteristic spacing comparable to the viscous compaction length (δ) and that the width of the channels varies inversely with the weakening caused by high fluid pressure. Because the channels have radial symmetry in 3-dimensions, the 2-D geometry of the model does not accurately capture the relation between metamorphic fluid production and channelized fluid flux. Aside from the fluid flux itself, this deficiency has the consequence that heat advection by the fluid; a cooling effect in the lower portion of the sill is not accurate. In the model, this effect is insignificant and earlier work (Connolly 1997b) suggests it would likewise be insignificant in 3-dimensional models.

The viscous compaction mechanism by power-law creep is thermally activated such that the effective solid viscosity, and therefore the viscous compaction length within the mush and the underlying rocks, can be expected to vary by at least six orders of magnitude due to temperature effects alone. After solid rheology, the initial porosity is the most important factor controlling the compaction length and time (τ) scales, specifically, $\delta \propto \sqrt{\phi}$ and $\tau \propto \delta\phi^2 \propto 1/\phi^{3/2}$ (Connolly and Podladchikov 2015). Given that the Bushveld Sill was emplaced in shallow-unmetamorphosed sediment, the initial porosity used here may underestimate the true porosity of the unmetamorphosed sediments by an order of magnitude. Such an underestimate would increase the length scale for compaction-generated processes by roughly a factor of three, while reducing their timescale by a factor of 0.03.

The present numerical simulation differs from previous models of channelized metamorphic fluid flow induced by decompaction weakening (Connolly 2010), in that the viscous mechanism is power-law rather than linear creep and that it accounts for the temperature dependence of the viscous mechanism. The latter detail has the consequence that the model has no intrinsic compaction length, although it is possible to evaluate the local compaction length. The numerical results of Figure 10 show that despite these differences, channelization does develop and, in the specific case considered, develops with a characteristic spacing of ~125 m. This

characteristic spacing is likely influenced by a number of factors that have not been investigated individually, but variations that increase the local compaction length and/or decrease the rate of devolatilization likely will increase the characteristic spacing. Because the channel-forming mechanism results in compaction of the surrounding rocks (Connolly and Podladchikov 2007), once the initial set of channels form then all subsequent fluid flow exploits the existing channels and, because the local compaction length decreases upwards due to the inverted thermal gradient, there is no tendency for the channels to coalesce. These generalizations assume a homogeneous metamorphic source. Strong source heterogeneity (*i.e.*, floor diapirs) would likely lead to flow events with larger spatial variability.

Likewise, this simulation differs from previous numerical models of diapirism in the Bushveld Complex (*e.g.*, Gerya and Yuen 2003). Their model relied on diapir nucleation at the site of a pre-existing anticlinal fold on the intrusion floor. Reducing the size of the fold reduced the size of the diapir or eliminated it altogether. Gerya and Yuen (2003) modelling of cold diapirism in layered intrusions thus suggest that without specific floor geometries (*i.e.*, high initial anticlines formed during initial magma intrusion), diapirism cannot develop. It is here suggested that the channelized flow of fluids released during dehydration melting or otherwise induce localized weakening of the floor rocks.

6.2 A qualitative model

A semi-quantitative model that combines the fluid transport numerical model and field observations noted here with the quantitative model of the thermal evolution of the Bushveld Complex and surrounding country rock by Cawthorn and Webb (2013) as well as the floor diapir formation model of Gerya *et al.* (2004) is shown in time sequence diagrams of Figure 11. Over time, this sill is allowed to both crystallize owing to heat loss out the bottom and top (forming a growing crystal pile at the base of the sill) and inflate to a final thickness of 8 km. The model is illustrated in four major steps (a-d in Figure 11). Figure 11a presents the initial condition of a 2 km thick sill injected 2 km below the surface. Following Gerya *et al.*, it is assumed the floor has topographical irregularities that form the sites of eventual dome/diapir formation. In Figure 11b, after 6,000 years, the sill has grown the 4 km thick and formed much of the Lower Zone. Heating and dehydration of the floor rocks lead to numerous fluid plumes percolating into the Lower Zone section (blue arrows). Injection of these fluids could give rise to the minor excursion in Sr and other isotopes seen in the Lower and Critical Zones.

After about 30,000 years Figure 11c, the sill has grown to 6 km thick. It is about this time that the maximum heating and dehydration of the floor rock occurs. Growth of the diapir leads to a preferential flow of fluid focused into the diapir and into the sill, resulting in the formation of a breccia pipe and injection of large volumes of fluid into the magma chamber above the crystal pile. Deformation of the crystal pile in response to the intrusion of the diapir starts to speed up (black arrow). Although not shown, it is assumed that fluid injection into the Bushveld chamber is minimal once the maximum extent of thermal heating and dehydration of the country rock is reached during crystallization of the Main Zone. New injections of magma during the crystallization of the Upper Zone pull the isotopic compositions back towards mantle compositions with only minimal country fluid contamination at this point.

After 180,000 years Figure 11d, growth of the sill is to 8 km and crystallization is complete (solid temperature profile). The intrusion continues to cool, however, and even after 580,000 years (dashed temperature profile) the floor rocks remain hot, allowing diapir growth to continue, but very little additional dehydration fluid is generated after about 30,000 years. Over time, the earlier formed pipes are pushed to the flanks of the diapir as the domes continue to intrude and deform the Bushveld Layered Series. As the system eventually cools, fractures and veins can form in the increasingly brittle rocks as temperatures fall below 700°C (Schiffries and Rye 1990).

In summary, heating of the Transvaal sediments resulted in a) generation of diapiric upwelling and b) generation of large volumes of fluid. The combined effect is that inflow of country fluids is focused by the developing domes, leading to continued fluid inflow into the growing dome even as the rocks themselves dehydrate. This inflow enhances both local melting of the country rock and the growth of the dome itself.

There are numerous caveats to the above model. For example, the filling of the magma chamber could be a continuous or aperiodic process. Aperiodic infilling and inflation of the Bushveld magma chamber can lead to relatively abrupt increases in the pressure in the underlying Transvaal sequence. The marked changes in isotopic composition of the Bushveld rocks noted in Figure 2 have been attributed to major periods of chamber growth (*e.g.*, Kruger 1990). However, the added weight of the Main Zone magma during rapid inflation of the Bushveld chamber could have triggered the sudden loss of over-pressured gas, in what one might consider to be the world's largest *whoopee cushion* effect.

The brecciation seen in the diatreme implies the top of the pipe had a free surface in which to expel the blocks. This is most readily accomplished by allowing the country

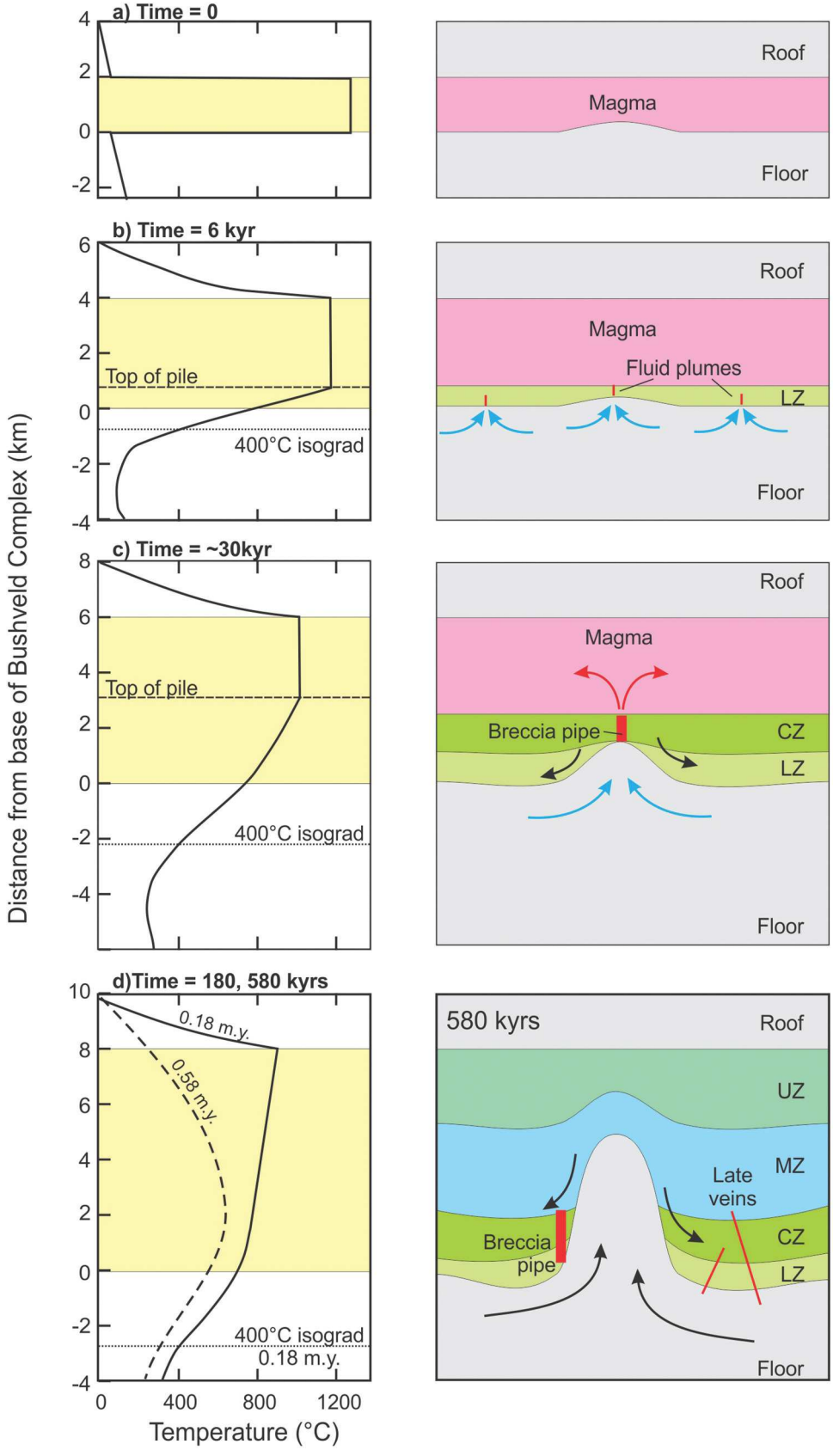

Figure 11. Semi-quantitative model of the thermal evolution of the Bushveld Complex and surrounding country rock, floor diapir formation, and breccia pipe emplacement at different times after initial emplacement as shown. Thermal evolution, inflation, and crystallization model is after Cawthorn and Webb (2013), diapir development is broadly after Gerya *et al*. (2004), and the quantitative model of fluid generation and transport of this study. Note that the maximum extent of the floor heating (and hence dehydration) occurs at about the same time the Main Zone begins to crystallize, and stays hot for at least a half million years.

fluids to reach the top of the crystal pile and enter the magma chamber. Evidence of melting of existing mush on the floor of the magma chamber suggested by Eales *et al*. (1988) might be one result of a lower liquidus temperature resulting from fluid-magma mixing. The formation of chromite as a restite mineral is another possible result of an incongruent hydration-induced partial melting event (*e.g*., Schannor *et al*. 2018). Deeper in the pile, infiltrating country fluids may be affected by the inherently anisotropic nature of layered intrusions and locally move laterally along more permeable layers.

For the country fluid, the main pathways into the chamber are primarily by channelled pipe-like porous flow that can be rapid enough to induce brecciation of the more solidified parts of the crystal pile at high temperatures where fluids are focused by floor structures such as the developing diapirs. Away from the channelled inflow of country fluids into the Bushveld Complex, the igneous rocks near the base of the intrusions may show little evidence of this fluid influx; the rock would preserve their initial isotopic signature, for example.

Finally, the fluid flow model shown in Figure 10 illustrates that the country fluid incursion produces highly permeable pipes that can have a horizontal flow component that can drain interstitial igneous fluids generated during the crystallization of the surrounding mush. This is supported by the work of Peyerl (1982), who noted that the PGE mineralogy in the surrounding host rock, particularly the distal chromitite layers, has been affected out to 1–2 km beyond the margins of the PGE-enriched pipes. This would suggest that the secondary dunite pipes and their associated PGE mineralization developed by the inflow of mineralizing fluid from the surrounding crystal pile largely as envisioned by Schiffries (1982).

7. The subduction zone connection

7.1 Subduction zone fluids and mantle diapirs

Subduction zones play a key role in the dynamics of the Earth, generating high-magnitude deep earthquakes and potentially transporting material to the mantle-core boundary. This system of recycling oceanic crust is linked to the origin and growth of continental crust (Rapp and Watson 1995) and signatures from subducted materials have been identified in fresh oceanic crust (Ben Othman *et al*. 1989). Further, the mantle is a major reservoir for H_2O. Estimates suggest subduction zones deliver six times more H_2O into the mantle than is released back at the surface by arc volcanism, with this subducted H_2O likely stored, in part, as a free fluid phase above 200–300 km depth, and bound entirely in minerals below this depth (Thompson 1992).

Subduction processes generate the melts that become arc volcanoes such as the 'Ring of Fire'. Study of the erupted materials at volcanic arcs provides much of the insight into slab dehydration and fluid circulation. Trace element and radiogenic isotope signatures both indicate a relatively large slab component, although trace-element measurements suggest a significantly higher amount of slab material than do isotopic signatures (Hawkesworth *et al*., 1993). Geochemistry of the NE Japan arc as well as numerical modelling of slab-fluid-fluxed melting in the mantle wedge demonstrate island arc volcanic activity is strongly driven by fluid-induced mantle melting (*e.g*., Kimura and Yoshida 2006). The geochemical signatures of fluids released from subducted slabs have been identified in other volcanic arc magmas worldwide (*e.g*. Kent and Elliott 2002; Bouvier *et al*. 2008). Additional numerical modelling suggests that even in arc materials that exhibit minimal to no trace element or isotopic slab signature, H_2O is required to generate island arc basalts (Ayers 1998). Slab fluids are estimated to migrate relatively quickly through the mantle wedge, with typical transfer times of approximately 30,000 to 120,000 years indicated by ^{238}U-^{230}Th disequilibrium (Hawkesworth 1997). While there is little doubt that the lithospheric slab dehydrates as it descends, it is uncertain as to how fluid escapes the subducted slab and migrates through the mantle wedge to generate melt. Several authors (*e.g*. Gerya and Yuen 2003; Marschall and Schumacher 2012) have suggested that the formation of buoyant mantle diapirs can allow for fluid addition into the mantle wedge, generating melt; it is suggested here that these diapirs are perhaps even more important in fluid focusing.

The conceptual model for diapirism in a subduction zone involves gravitational instabilities forming along a thin, buoyant layer at the surface of the subducting slab. These instabilities then detach and rise through the mantle wedge. This was modelled in two dimensions by Gerya and Yuen (2003); examples are shown in Figure 12. They model a scenario in which cold, less dense plumes emerge from the slab surface due to Rayleigh–Taylor instabilities (the same process noted above which can produce diapirs at the Bushveld Complex; Gerya *et al*. 2004). The slab mélange, a mixture of hydrated peridotite, sedimentary rock, and altered oceanic crust, is less dense than the asthenosphere (although temperature differences slightly offset density differences). Their model finds like upwellings of cold, less dense material into hot, dense material are geodynamically feasible. An expanded model (Gerya *et al*., 2006) incorporates the thermodynamic effects of slab dehydration, metamorphic reactions, and mantle melting. This model suggests that two types of plumes may form: mixed, which

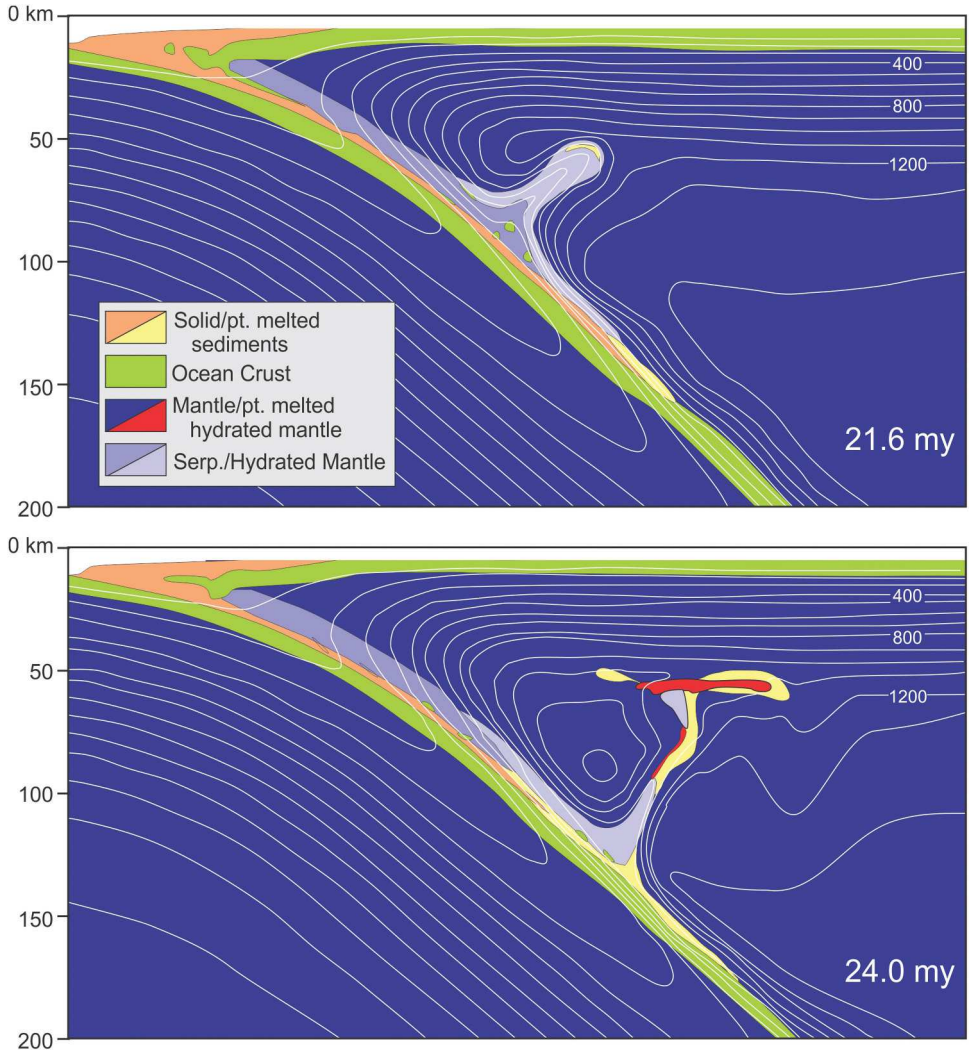

Figure 12. Examples of modelled mantle diapirs, showing the variation in morphology of 'cold plumes' for two variation of model parameters in numerical experiments with high initial buoyancy. Redrawn and simplified after.Gerya and Yuen (2003)

initiate from the slab and entrain both slab and mantle materials, and unmixed, which initiate from the mantle due to slab-derived fluid infiltration. This may explain the variations in volcanic arc magma signatures; arc magmas with crustal melt signatures may derive from mixed plumes, while those with fluid signatures originate from unmixed plumes. Gerya *et al*. (2006) also note the similarity to Bushveld Complex diapirs, although they discuss these diapirs in the context of heat rather than fluid transport. Their model was expanded to three dimensions (Zhu *et al*. 2009) and found great similarity to the distribution of volcanoes in the subduction zone of northeastern Japan. Zhu *et al*. note that plume shape and growth are strongly a function of mantle viscosity, a value which is not well constrained near the plate boundary.

More in-depth modelling is conducted on diapir formation in subduction zones by Marschall and Schumacher (2012). They explore in detail the possibility that mélange zones could be responsible for the combined altered oceanic crust, sedimentary, and depleted mantle signatures in erupted arc magmas. Using results from field investigations of exhumed mélange zones, numerical modelling, geophysics, and geochemistry, they produce a conceptual model for the formation of diapirs in subduction zones. In this model, mélange is formed; its low mechanical strength leads to instabilities and the development of buoyant diapirs, which rise into the hot corner of the mantle wedge, dehydrate, melt, and generate fluid and melt compositions which are ultimately the source of plutons and surface volcanoes. This model suggests that the trajectories of plumes as they rise would not necessarily be vertical but may be impacted by corner flow and move obliquely away from the trench. This presents a solution to a number of questions raised by other models: it explains the location

of the volcanic forearc as well as the source of the trace-element signatures in erupted materials.

Investigations into diapir formation have utilized geochemistry in addition to the geophysical and numerical methods highlighted above. One major concern for the viability of the diapir model is the time it would take for a plume to rise. Based on ^{10}Be and U-Th isotope systematics, the timescale of a subduction cycle is well established. Hall and Kincaid (2001) experimentally simulated subduction-driven flow and buoyant mantle flow with two solutions of different densities to understand the growth of instabilities. Their results suggest the rapid transport times dictated by isotopic results would be feasible under the diapir model. Cruz-Uribe *et al*. (2018), drawing on the conceptual model of Marschall and Schumacher (2012), found that partially melted mélange materials injected as part of the diapir could account for the geochemical signatures of erupted arc materials. The conclusion that mantle wedge plumes could account for the petrology of arc melts is supported by other authors as well (*e.g*., Castro *et al*. 2010).

7.2 The Bushveld Complex as an analogue for subduction zone hydrothermal systems

The stratigraphic sequence of a footwall of unmetamorphosed sediments overlain by an ultramafic sequence of olivine + pyroxene bearing rocks of the Lower Zone of the Bushveld Complex is broadly analogous to the mafic lithosphere slab ± sediments subducting beneath an ultramafic mantle wedge. In both instances, footwall rocks may rise as diapirs into overlying ultramafic rock. The Bushveld evidence noted above illustrates that fluid released by heating of the underlying rock can be effectively focused by the diapirs, allowing for rapid inflow into the growing crystal pile. This can allow for the fluid to retain its isotopic and composition signature of the descending slab (in the subduction case) or that of the underlying Transvaal sediments (in the case of the Bushveld Complex).

There are, of course, differences in the two environments. This includes the fact that subducting slabs has a pronounced dip as compared with the presumed initially sub-horizontal lower contact of the Bushveld with the country rock, which likely did not develop its modest dip until the generation by lower crustal melting and intrusion of the Bushveld Granite by the same thermal anomaly that produced the Bushveld magma. The model (Figure 10) demonstrates that even without this dip, the diapirs can channel fluids to move vertically. Furthermore, the rapid fluid influx into the Bushveld magma chamber allowed space for brecciation of the fluid channelway. Perhaps most significantly, slab fluids are largely incorporated into any mantle melt generated. The eruption of this melt provides direct inference of the fluid composition. In contrast, the fluid addition and silicate melt produced by hydration melting in the Bushveld system can be diluted by mixing with large volumes of pre-existing magma, which then is only recorded by the later precipitated solid assemblage. Thus, country fluid signatures in Bushveld diapirs may be weaker than they would appear in a mantle melt generated by a subduction zone diapir.

With these caveats, however, large sills such as the Bushveld Complex can act as proxies for dehydration processes in subduction zones, allowing one to observe in the field how country fluids can migrate into hotter rocks and to identify how their geochemical and isotopic characteristics might be altered or not as it does so. The diapir model is not the only model for subduction zone fluid release and migration; identifying geochemical and isotopic alterations due to fluid influx at Bushveld may help to further understand how viable the diapir model is in subduction zones. Additionally, the diatreme and other pipe-like bodies of the Bushveld Complex suggest that fluid influx into the mantle wedge can be unusually voluminous and rapid, following an extended period of fluid overpressure build-up and its sudden release. This rapid fluid transport allows the slab fluids to retain much of their geochemical characteristics as they quickly move into the mantle wedge. A corresponding build-up of fluid overpressure and periodic release of vapour into the hotter parts of the mantle wedge would suggest that hydration melting in subduction zones is periodic and not continuous. The periodic nature of arc magmatism may, in part, reflect this intermittent fluid influx.

A common objection to the idea that country fluids have contaminated the Bushveld magma is the presence of Mississippi Valley-type deposits in the Transvaal Supergroup and other evidence noted above imply that all of the country fluids migrated laterally and not up into the intrusion. However, it is noted that models of fluid flow in subduction zones show a combination of fluid flow both along the dipping subducting plate (where it may reach the forearc regions) as well as vertical and into the overlying mantle.

8. Conclusions

The Bushveld Complex is apparently unique in that it was intruded relatively rapidly as a thick sill into an unmetamorphosed sedimentary sequence, leading to the formation of a wide basal aureole and the generation of voluminous amounts of metamorphic fluids. The most pronounced expression of this is the formation of diapiric structures in the thicker parts of the Bushveld and

evidence for fluid focusing in these structures by the presence of diatremes and other pipe-like bodies of a size and character unique to the Bushveld Complex. These bodies and numeric modelling results suggest that much of the country fluid influx is focused by the diapirs structures into pipe-like channels. Rapid influx of country fluid into the magma chamber can affect the crystallization behaviour and isotopic character of the resident magma.

The thermal profile and lithologic sequence of the Bushveld Complex and the underlying country rock are similar to that seen in subduction zones. Understanding the degree that country fluids can retain their geochemical and isotopic character as they percolate through thick sequences of Bushveld ultramafic and mafic rock has implications for slab fluids. The results here suggest that fluids can retain their initial geochemical characteristics by periodic, rapid migration through overlying rock. In this regard, studies of the geochemical and isotopic character of late-crystallizing Bushveld minerals and comparisons with intrusions that intruded drier country rocks may prove enlightening. More broadly, the merger of two major fields of igneous petrology and geochemistry, layered intrusions and subduction zone magmatism, will be of benefit to both.

Acknowledgments

This work was supported by NSF Grant EAR 1647727 to A. Boudreau. It was improved by reviews of an earlier draft by two anonymous reviewers.

Disclosure statement

No potential conflict of interest was reported by the authors.

Funding

This work was supported by the National Science Foundation [EAR 1647727].

References

Ayers, J., 1998, Trace element modeling of aqueous fluid-peridotite interaction in the mantle wedge of subduction zones: Contributions to Mineralogy and Petrology, v. 132, p. 390–404. doi:10.1007/s004100050431

Barnes, S.J., 1989, Are Bushveld U-type parent magmas boninites or contaminated komatiites?: Contributions to Mineralogy and Petrology, v. 101, p. 447–457. doi:10.1007/BF00372218

Barry, T.L., Pearce, J.A., Leat, P.T., Millar, I.L., and le Roex, A.P., 2006, Hf isotope evidence for selective mobility of high-field-strength elements in a subduction setting: South Sandwich Islands: Earth and Planetary Science Letters, v. 252, p. 223–244.

Barton, E.S., and Hallbauer, D.K., 1996, Trace-element and U-Pb isotope compositions of pyrite types in the Proterozoic Black Reef, Transvaal Sequence, South Africa: Implications on genesis and age: Chemical Geology, v. 133, p. 173–199. doi:10.1016/S0009-2541(96)00075-7

Ben Othman, D., White, W.M., and Patchett, J., 1989, The geochemistry of marine sediments, island arc magma genesis, and crust-mantle recycling: Earth and Planetary Science Letters, v. 94, p. 1–21. doi:10.1016/0012-821X(89)90079-4

Boorman, S.L., McGuire, J.B., Boudreau, A.E., and Kruger, F.J., 2003, Fluid overpressure in layered intrusions, part II: Formation of a breccia pipe in the eastern Bushveld Complex, Republic of South Africa: Mineralium Deposita, v. 38, p. 356–369. doi:10.1007/s00126-002-0312-5

Bouvier, A.-S., Métrich, N., and Deloule, E., 2008, Slab-derived fluids in the magma sources of St.Vincent (lesser antilles arc): Volatileand light element imprints: Journal of Petrology, v. 49, p. 1427–1448. doi:10.1093/petrology/egn031

Buick, I.S., Gibson, R.L., Cartwright, I., Maas, R., Wallmach, T., and Uken, R., 2000, Fluid flow in metacarbonates associated with emplacement of the Bushveld Complex, South Africa: Journal of Geochemical Exploration, v. 69–70, p. 391–395.

Buick, I.S., Maas, R., and Gibson, R. 2001. Precise U-Pb titanite age constraints on the emplacement of the Bushveld Complex, South Africa. Journal of the Geological Society 158:3–6. doi: 10.1144/jgs.158.1.3 1

Button, A., 1978, Diapiric structures in the Bushveld: Northeastern Transvaal, University of Witwatersrand Information Circular 123.

Cameron, E.N., 1978, The lower zone of the Eastern Bushveld Complex in the Olifants river trough: Journal of Petrology, v. 19, p. 437–462. doi:10.1093/petrology/19.3.437

Castro, A., Gerya, T., Garcia-Casco, A., Fernandez, C., Diaz-Alvarado, J., Moreno-Ventas, I., and Low, I., 2010, Melting relations of MORB-sediment melanges in underplated mantle wedge plumes; Implications for the Origin of cordilleran-type batholiths: Journal of Petrology, v. 51, p. 1267–1295. doi:10.1093/petrology/egq019

Cawthorn, R.G., Harris, C., and Kruger, F.J., 2000, Discordant ultramafic pegmatoidal pipes in the Bushveld Complex: Contributions to Mineralogy and Petrology, v. 140, p. 119–133. doi:10.1007/s004100000175

Cawthorn, R.G. and Webb, S.J., 2013, Cooling of the Bushveld Complex, South Africa: Implications for paleomagnetic reversals: Geology, v. 41, no. 6, p. 687–690. doi: 10.1130/G34033.1

Chutas, N.I., Bates, E., Prevec, S A.., Coleman, D., and Boudreau, A.E., 2012, Sr and Pb isotopic disequilibrium between coexisting plagioclase and orthopyroxene in the Bushveld Complex, South Africa: microdrilling and progressive leaching evidence for sub-liquidus contamination within a crystal mush. Africa: Contributions to Mineralogy and Petrology, v. 163 p. 653–668. doi: 10.1007/s00410-011-0691-7 4

Clarke, B.M., Uken, R., Watkeys, M.K., and Reinhardt, J., 2005, Folding of the Rustenburg layered suite adjacent to the steelpoort pericline: Implications for syn-Bushveld tectonism in the eastern Bushveld Complex: South African Journal of Geology, v. 108, p. 397–412. doi:10.2113/108.3.397

Connolly, J.A.D., 1997a, Devolatilization-generated fluid pressure and deformation-propagated fluid flow during

prograde regional metamorphism: Journal of Geophysical ResearchSolid Earth, v. 102, no. B8, p. 18149–18173.
Connolly, J.A.D., 1997b, Mid-crustal focused fluid movement: Thermal consequences and silica transport, *in* Jamtveit, B., and Yardley, B.W.D., eds., Fluid flow and transport in rocks: Mechanisms and effects: London, Chapman & Hall, 235–250 p. doi:10.1007/978-94-009-1533-6_14
Connolly, J.A.D., 2010, The Mechanics of Metamorphic Fluid Expulsion: Elements, v. 6, no. 3, p. 165–172.
Connolly, J.A.D. and Podladchikov, Y.Y., 2007, Decompaction weakening and channeling instability in ductile porous media: Implications for asthenospheric melt segregation: Journal of Geophysical Research: Solid Earth, v. 112, no. B10, p. 15. doi:10.1029/2005JB004213
Connolly, J.A.D. and Podladchikov, Y.Y., 2013, A hydromechanical model for lower crustal fluid flow, in Harlov, D.E., and AustrheimH, D.E., eds., Metasomatism and the chemical transformation of rock, lecture notes in Earth System Sciences: Verlag Berlin Heidelberg, Springer, 599–658 p. doi: 10.1007/978-3-642-28394-9_14
Connolly, J.A.D., and Podladchikov, Y.Y., 2015, An analytical solution for solitary porosity waves: Dynamic permeability and fluidization of nonlinear viscous and viscoplastic rock: Geofluids, v. 15, no. 1–2, p. 269–292.
Cruz-Uribe, A.M., Marschall, H.R., Gaetani, G.A., and Le Roux, V., 2018, Generation of alkaline magmas in subduction zones by partial melting of mélange diapirs—An experimental study: Geology, v. 46, p. 343–346. doi:10.1130/G39956.1
Dobson, P.F., and O'Neil, J.R., 1987, Stable isotope compositions and water contents of boninite series volcanic rocks from Chichi-jima, Bonin islands, Japan: Earth and Planetary Science Letters, v. 82, p. 75–86. doi:10.1016/0012-821X(87)90108-7
Eales, H.V., and Cawthorn, R.G., 1996, The Bushveld Complex, *in* Cawthorn, R.G., ed., Layered intrusions: Amsterdam, Elsevier, 181–229 p.
Eales, H.V., Field, M., De Klerk, W.J., and Scoon, R.N., 1988, Regional trends of chemical variation and thermal erosion in the Upper Critical Zone, Western Bushveld Complex: Mineralogical Magazine, v. 52, p. 63–79. doi: 10.1180/minmag.1988.052.364.06 364
Eiler, J.M., 2001, Oxygen isotope variations of basaltic lavas and upper mantle rocks: Reviews in Mineralogy and Geochemistry, v. 43, p. 319–364.
Eriksson, P.G., Hattingh, P.J., and Altermann, W., 1995, An overview of the geology of the Transvaal Sequence and Bushveld Complex, South Africa: Mineralium Deposita, v. 30, p. 98–111. 2 doi:10.1007/BF00189339
Eriksson, P.G., Schweitzer, K., Bosch, P.J.A., Schereiber, U.M., Van Deventer, J., and Hatton, C.J., 1993, The transvaal sequence: An overview: Journal of African Earth Science, v. 16, p. 25–51. doi:10.1016/0899-5362(93)90160-R
Farquhar, J. and Wing, B.A., 2003, Multiple sulfur isotopes and the evolution of the atmosphere: Earth and Planetary Science Letters, v. 213, p. 1–13. doi: 10.1016/S0012-821X(03)00296-6
Farquhar, J., Wing, B.A., McKeegan, K.D., Harris, J.W., Cartigny, P., and Thiemens, M.H., 2002, Mass-independent Sulfur of inclusions in Diamond and Sulfur recycling on early earth: Science, v. 298, p. 2369–2372. doi: 10.1126/science.1078617
Ferguson, J., and McCarthy, T.S., 1970, Origin of an ultramafic pegmatoid in the eastern part of the Bushveld Complex: Geological Society of South Africa Special Publication, v. 1, p. 74–79.
Finn, C.A., Bedrosian, P.A., Cole, J.C., Khoza, D.T., and Webb, S.J., 2015, Mapping the 3D extent of the Northern Lobe of the Bushveld layered mafic intrusion from geophysical data: Precambrian Research, v. 268, p. 279–294. doi:10.1016/j.precamres.2015.07.003
Gerya, T.V., Connolly, James A.D.., Yuen, D.A., Gorczyk, W., and Capel, A.M., 2006, Seismic implications of mantle wedge plumes: Physics of the Earth and Planetary Interiors, v. 156, p. 59–74. doi: 10.1016/j.pepi.2006.02.005 1-2
Gerya, T.V., Uken, R., Reinhardt, J., Watkeys, M.K., Maresch, W.V., and Clarke, B.M., 2003, Cold fingers in hot magma: Numerical modeling of country-rock diapirs in the Bushveld Complex, South Africa: Geology, v. 31, no. 9, p. 753–756. doi: 10.1130/G19566.1
Gerya, T.V., Uken, R., Reinhardt, J., Watkeys, M.K., Maresch, W.V., and Clarke, B.M., 2004, "Cold" diapirs triggered by intrusion of the Bushveld Complex: Insight from two-dimensional numerical modeling, in special paper 380: Gneiss Domes in Orogeny, Geological Society of America, v. 380, p. 117–127. doi:10.1130/0-8137-2380-9.117
Gerya, T.V., and Yuen, D.A., 2003, Rayleigh–Taylor instabilities from hydration and melting propel 'cold plumes' at subduction zones: Earth and Planetary Science Letters, v. 212, p. 47–62. doi:10.1016/S0012-821X(03)00265-6
Gleason, J.D., Gutzmer, J., Kesler, S.E., and Zwingmann, H., 2011, 2.05-Ga isotopic ages for transvaal mississippi valley–type deposits: Evidence for large-scale hydrothermal circulation around the Bushveld Igneous Complex: South African Journal of Geology, v. 119, p. 69–80.
Günther, T., Haase, K., Junge, M., Oberthür, T., Woelki, D., and Krumm, S., 2018, Oxygen isotope and trace element compositions of platiniferous dunite pipes of the Bushveld Complex, South Africa–Signals from a recycled mantle component? Lithos 310, 332–341. doi:10.1016/j.lithos.2018.04.017
Hall, P.S., and Kincaid, C., 2001, Diapiric flow at subduction zones: A recipe for rapid transport: Science, v. 292, p. 2472–2475. doi: 10.1126/science.1060488
Hanley, J.J., Mungall, J.E., Pettke, T., Spooner, E.T.C., and Bray, C. J., 2005, Ore metal redistribution by hydrocarbon-brine and hydrocarbon-halide melt phases, North Range footwall of the Sudbury Igneous Complex, Ontario, Canada: Mineralium Deposita, v. 40, p. 237–256. doi: 10.1007/s00126-005-0004-z
Harmer, R.E., Auret, J.M., and Eglington, B.M., 1995, Lead isotope variations within the Bushveld Complex, Southern Africa: A reconnaissance study: Journal of African Earth Science, v. 21, p. 595–606. doi:10.1016/0899-53629500109-3
Harmer, R.E. and Sharpe, M.R., 1985, Field Relations and Strontium Isotope Systematics of the Marginal Rocks of the Eastern Bushveld Complex: Economic Geology, v. 80, p. 813–837 doi: 10.2113/gsecongeo.80.4.813 4
Harris, C., and Chaumba, J.B., 2001, Crustal contamination and the fluid-rock interaction during the formation of the Platreef, Northern limb of the Bushveld Complex, South Africa: Journal of Petrology, v. 42, p. 1321–1347. doi:10.1093/petrology/42.7.1321
Harris, C., Pronost, J.J.M., Ashwal, L.D., and Cawthorn, R.G., 2005, Oxygen and Hydrogen Isotope Stratigraphy of the Rustenburg Layered Suite, Bushveld Complex: Constraints on Crustal Contamination: Journal of Petrology, v. 46, p. 579–601. doi: 10.1093/petrology/egh089 3

Harris, N., McMillan, A., Holness, M., Uken, R., Watkeys, M., Rogers, N., and Fallick, A., 2003, Melt generation and fluid flow in the thermal aureole of the Bushveld Complex: Journal of Petrology, v. 44, p. 1031–1054. doi:10.1093/petrology/44.6.1031

Hatton, C.J., and Sharpe, M.R., 1989, Significance and origin of boninite-like rocks associated with the Bushveld Complex, *in* Crawford, A.J., ed., Boninites and related rocks: London, Unwin Hyman, 174–208 p.

Hawkesworth, C.J., 1997, U-Th isotopes in arc magmas: Implications for element transfer from the subducted crust: Science, v. 276, p. 551–555. doi:10.1126/science.276.5312.551

Hawkesworth, C.J., Gallagher, K., Hergt, J.M., and McDermott, F., 1993, Mantle and slab contributions in ARC magmas: Annual Review of Earth and Planetary Sciences, v. 21, p. 175–204. doi: 10.1146/annurev.ea.21.050193.001135 1

Hildreth, W., Halliday, A.N., and Christianson, R.L., 1991, Isotopic and chemical evidence concerning the genesis and contamination of basaltic and rhyolitic magma beneath the yellowston plateau volcanic field: Journal of Petrology, v. 32, p. 63–138. doi:10.1093/petrology/32.1.63

Ireland, R.H.P., and Penniston-Dorland, S.C., 2015, Chemical interactions between a sedimentary diapir and surrounding magma: Evidence from the phepane dome and Bushveld Complex, South Africa: American Mineralogist, v. 100, p. 1985–2000. doi:10.2138/am-2015-5196

Irvine, T.N., 1977, Chromite crystallization in the join Mg2SiO4-CaMgSi2O6-CaAl2Si2O8-MgCr2O4-SiO2: Washington, D.C.: Carnegie Institute of Washington Yearbook 76, p. 465–472 p.

Ito, E., Harris, D.M., and Anderson, A.T., 1983, Alteration of oceanic crust and geologic cycling of chlorine and water: Geochimica Et Cosmochimica Acta, v. 47, p. 1613–1624. doi:10.1016/0016-7037(83)90188-6

Ito, E. and Stern, R.J., 1986, Oxygen- and strontium-isotopic investigations of subduction zone volcanism: the case of the Volcano Arc and the Marianas Island Arc: Earth and Planetary Science Letters, v. 76, p. 312–320. 3-4 doi:10.1016/0012-821X(86)90082-8

Jahn, B.-M., Bertrand-Sarfati, J., Morin, N., and Mace, J., 1990, Direct dating of stromatolitic carbonates from the schmidtsdrif formation (Transvaal Dolomite), South Africa, with implications on the age of the ventersdorp supergroup: Geology, v. 18, p. 1211–1214. doi:10.1130/0091-76131990018<1211:DDOSCF>2.3.CO;2

Johnson, T., Brown, M., Gibson, R., and Wing, B., 2004, Spinel-cordierite symplectites replacing andalusite: Evidence for melt-assisted diapirism in the Bushveld Complex, South Africa: Diapirism in the Bushveld Complex: Journal of Metamorphic Geology, v. 22, p. 529–545. doi:10.1111/j.1525-1314.2004.00531.x

Kent, A.J.R., and Elliott, T.R., 2002, Melt inclusions from marianas arc lavas: Implications for the composition and formation of island arc magmas: Chemical Geology, v. 183, p. 263–286. doi:10.1016/S0009-2541(01)00378-3

Kimura, J.-I., and Yoshida, T., 2006, Contributions of slab fluid, mantle wedge and crust to the Origin of quaternary lavas in the NE Japan arc: Journal of Petrology, v. 47, p. 2185–2232. doi:10.1093/petrology/egl041

Kinnaird, J.A., Kruger, F.J., Nex, P.A.M., and Cawthorn, R.G., 2002, Chromitite formation - a key to understanding processes of platinum enrichment: Transactions of the Institute of Mining and Metallurgy B, v. 111, p. B23–B35.

Kruger, F.J., 1990, The stratigraphy of the Bushveld Complex: A reappraisal and the relocation of the Main Zone boundaries: South African Journal of Geology, v. 93, p. 376–381.

Kruger, F.J., 2005, Filling the Bushveld Complex magma chamber: Lateral expansion, roof and floor interaction, magmatic unconformities, and the formation of giant chromitite, PGE and Ti-V-magnetitite deposits: Mineralium Deposita, v. 40, no. p, p. 451–472. doi:10.1007/s00126-005-0016-8

Kyser, T.K., Cameron, W.E., and Nisbet, E.G., 1986, Boninite petrogenesis and alteration history: constraints from stable isotope compositions of boninites from Cape Vogel, New Caledonia and Cyprus: Contributions to Mineralogy and Petrology, v. 93, p. 222–226. doi: 10.1007/BF00371324 2

Kyser, T.K., and O'Neil, J.R., 1984, Hydrogen isotope systematics of submarine basalts: Geochimica Et Cosmochimica Acta, v. 48, p. 2123–2133. doi:10.1016/0016-70378490392-2

Labidi, J., Cartigny, P., Birck, J.L., Assayag, N., and Bourrand, J.J., 2012, Determination of multiple sulfur isotopes in glasses: A reappraisal of the MORB $\delta^{34}S$: Chemical Geology, v. 334, p. 189–198. doi:10.1016/j.chemgeo.2012.10.028

Lahaye, Y., and Arndt, N., 1996, Alteration of a komatiite flow from Alexo, Ontario, Canada: Journal of Petrology, v. 37, p. 1261–1294. doi: 10.1093/petrology/37.6.1261

Leeman, W.P., and Hawkesworth, C.J., 1986, Open magma systems: Trace element and isotopic constraints: Journal of Geophysical Research, v. 91, no. B6, p. 5901–5912. doi:10.1029/JB091iB06p05901

Letts, S., Torsvik, T.H., Webb, S.J., and Ashwal, L.D., 2009, Palaeomagnetism of the 2054 ma Bushveld Complex (South Africa): Implications for emplacement and cooling: Geophysical Journal International, v. 179, no. 2, p. 850–872.

Løseth, H., Wensaas, L., Arntsen, B., Hanken, N.-M., Basire, C., and Graue, K., 2011, 1000 m long gas blow-out pipes: Marine and Petroleum Geology, v. 28, p. 1047–1060. doi:10.1016/j.marpetgeo.2010.10.001

Magalhães, N., Penniston-Dorland, S., Farquhar, J., and Mathez, E.A., 2018, Variable sulfur isotope composition of sulfides provide evidence for multiple sources of contamination in the Rustenburg Layered Suite. Bushveld Complex: Earth and Planetary Science Letters, v. 492, p. 163-173. doi:10.1016/j.epsl.2018.04.010

Maier, W.D., Arndt, N.T., and Curl, E.A., 2000, Progressive crustal contamination of the Bushveld Complex: Evidence from Nd isotopic analysis of the cumulate rocks: Contributions in Mineralogy and Petrology, v. 140, p. 316–327. doi:10.1007/s004100000186

Marschall, H.R., and Schumacher, J.C., 2012, Arc magmas sourced from mélange diapirs in subduction zones: Nature Geoscience, v. 5, p. 862–867. doi:10.1038/ngeo1634

Mathez, E.A., Agrinier, P., and Hutchinson, R., 1994, Hydrogen isotope composition of the merensky reef and related Rocks, Atok Section, Bushveld Complex: Economic Geology, v. 89, p. 791–802. doi: 10.2113/gsecongeo.89.4.791

Mathez, E.A., and Kent, A.J.R., 2007, Variable initial Pb isotopic compositions of rocks associated with the UG2 chromitite, eastern Bushveld Complex: Geochimica Et Cosmochimica Acta, v. 71, p. 5514–5527 doi:10.1016/j.gca.2007.09.014

Mathez, E.A. and Waight, T.E., 2003, Lead isotopic disequilibrium between sulfide and plagioclase in the Bushveld Complex and the chemical evolution of large layered intrusions. Geochimica et Cosmochimica Acta v. 67, p. 1875–1888. doi: 10.1016/S0016-7037(02)01294-2

McCandless, T.E., Ruiz, J., Adair, B.I., and Freydier, C., 1999, Re-Os isotope and Pd/Ru variations in chromitites from the Critical zone, Bushveld Complex, South Africa: Geochimica Et Cosmochimica Acta, v. 63, p. 911–923. doi:10.1016/S0016-70379900092-7

Nielson, S.G., Shimizu, N., Lee, C.-T.A., and Behn, M.D., 2014, Chalcophile behavior of thallium during MORB melting and implications for the sulfur content of the mantle: Geochemistry, Geophysics, Geosystems, v. 15, p. 4905–4919. doi:10.1002/2014GC005536

Nohda, S., and Wasserburg, G.J., 1981, Nd and Sr isotopic study of volcanic rocks from Japan: Earth and Planetary Science Letters, v. 52, p. 264–276. doi:10.1016/0012-821X8190181-3

Penniston-Dorland, S.C., Mathez, E.A., Wing, B.A., Farquhar, J., and Kinnaird, J.A., 2012, Multiple sulfur isotope evidence for surface-derived sulfur in the Bushveld Complex: Earth and Planetary Science Letters, v. 337-338, p. 236–242. doi: 10.1016/j.epsl.2012.05.013

Penniston-Dorland, S.C., Wing, B.A., Nex, P.A.M., Kinnaird, J.A., Farquhar, J., Brown, M., and Sharman, E.R., 2008, Multiple sulfur isotopes reveal a magmatic origin for the platreef platinum group element deposit, Bushveld Complex, South Africa: Geology, v. 36, no. 12, p. 979–982. doi:10.1130/G25098A.1

Peyerl, W.J., 1982, The influence of the Driekop dunite pipe on the platinum-group mineralogy of the UG-2 chromitite in its vicinity: Economic Geology, v. 77, p. 1432–1438. doi:10.2113/gsecongeo.77.6.1432

Pokrovski, G.S., Roux, J., and Harrichoury, J.-C., 2005, Fluid density control on vapor-liquid partitioning of metals in hydrothermal systems: Geology, v. 33, no. 8, p. 657–660. doi:10.1130/G21475AR.1

Prevec, S.A., Ashwal, L.D., and Mkaza, M.S., 2005, Mineral disequilibrium from the merensky pegmatoid, western Bushveld Complex, South Africa: New Sm–Nd isotopic evidence: Contributions to Mineralogy and Petrology, v. 149, p. 306–315. doi:10.1007/s00410-005-0650-2

Pronost, J., Harris, C., and Pin, C. 2008. Relationship between footwall composition, crustal contamination, and fluid-rock interaction in the Platreef, Bushveld Complex, South Africa. Mineralium Deposita 43:825–848. doi:10.1007/s00126-008-0203-5

Raedeke, L.D., and McCallum, I.S., 1984, Investigations in the stillwater Complex: Part II. Petrology and petrogenesis of the ultramafic series: Journal of Petrology, v. 25, p. 395–420. doi:10.1093/petrology/25.2.395

Rapp, R.P., and Watson, E.B., 1995, Dehydration melting of metabasalt at 8-32 kbar: Implications for continental growth and crust-mantle recycling: Journal of Petrology, v. 36, p. 891–931. doi:10.1093/petrology/36.4.891

Reid, D.L., and Basson, I.J., 2002, Iron-rich ultramafic pegmatite replacement bodies within the Upper Critical zone, Rustenburg Layered Suite, Northam Platinum Mine, South Africa: Mineralogical Magazine, v. 66, p. 895–914. doi:10.1180/0026461026660066

Ripley, E.M., Park, Y.-R., Li, C., and Naldrett, A.J., 1999, Sulfur and oxygen isotopic evidence of country rock contamination in the Voisey's Bay Ni-Cu-Co deposit, Labrador, Canada: Lithos, v. 47, p. 53–68. doi:10.1016/S0024-49379900007-9

Roelofse, F., and Ashwal, L.D. 2008. Symplectitic augite from the Platreef-textural evidence for fluid/rock interaction in the Northern Sector of the Northern Limb of the Bushveld Complex? Contributions to Mineralogy and Petrology. 111:21–26. doi:10.2113/gssajg.111.1.21

Roelofse, F. and Ashwal, L.D., 2012, The Lower Main Zone in the Northern Limb of the Bushveld Complex—a >1.3 km thick sequence of intruded and variably contaminated crystal mushes: Journal of Petrology, v. 53, p. 1449–1476. doi: 10.1093/petrology/egs022

Roelofse, F., Ashwal, L.D., and Romer, R.L., 2015, Multiple, isotopically heterogeneous plagioclase populations in the Bushveld Complex suggest mush intrusion: Geochemistry, v. 75, p. 357–364. doi: 10.1016/j.chemer.2015.07.001 3

Schannor, M., Veksler, I.V., Hecht, L., Harris, C., Romer, R.L., and Manyeruke, T.D., 2018, Small-scale Sr and O isotope variations through the UG2 in the eastern Bushveld Complex: The role of crustal fluids: Chemical Geology, v. 485, p. 100–112.

Schiffries, C.M., 1982, The petrogenesis of a platiniferous dunite pipe in the Bushveld Complex: Infiltration metasomatism by a chloride solution: Economic Geology, v. 77, p. 1439–1453.

Schiffries, C.M. and Rye, D.M., 1989, Stable isotopic systematics of the Bushveld Complex: I. Constraints of magmatic processes in layered intrusions: American Journal of Science, v. 289, p. 841–873. doi: 10.2475/ajs.289.7.841

Schiffries, C.M., and Rye, D.M., 1990, Stable isotopic systematics of the Bushveld Complex: II. Constraints on hydrothermal processes in layered intrusions: American Journal of Science, v. 290, p. 209–245. doi:10.2475/ajs.290.3.209

Schiffries, C.M. and Skinner, B.J., 1987, The Bushveld hydrothermal system; field and petrologic evidence: American Journal of Science, v. 287, p. 566–595. doi: 10.2475/ajs.287.6.566

Scoon, R.N., and Costin, G., 2018, Chemistry, morphology and origin of magmatic-reaction chromite stringers associated with anorthosite in the Upper Critical Zone at Winnaarshoek, Eastern Limb of the Bushveld Complex: Journal of Petrology, v. 59, no. 8, p. 1551–1578.

Scoon, R.N. and Mitchell, A.A., 2004, The platiniferous dunite pipes in the eastern limb of the Bushveld Complex: Review and comparison with unmineralized discordant ultramafic bodies: South African Journal of Geology, v. 107, p. 505–520. doi: 10.2113/gssajg.107.4.505

Sharman-Harris, E.R., Kinnaird, J.A., Harris, C., and Horstmann, U.E., 2005, A new look at sulphide mineralization in the northern limb, Bushveld Complex: A stable isotope study: Applied Earth Science IMM Transactions Section B, v. 114, p. B252–B263.

Sharpe, M.R., 1981, The chronology of magma influxes to the eastern compartment of the Bushveld Complex as exemplified by its marginal border groups: Journal of the Geological Society, v. 138, p. 307–326.

Sharpe, M.R., 1985, Strontium isotope evidence for preserved density stratification in the Main Zone of the Bushveld Complex, South Africa: Nature, v. 316, p. 119–126. doi: 10.1038/316119a0 6024

Shaw, A.M., Hauri, E.H., Fischer, T.P., Hilton, D.R., and Kelley, K.A., 2008, Hydrogen isotopes in Mariana arc melt inclusions: Implications for subduction dehydration and the deep-Earth water cycle: Earth and Planetary Science Letters, v. 275, p. 138–145. doi:10.1016/j.epsl.2008.08.015

Shieh, Y.N., and Taylor, H.P., 1969, Oxygen and hydrogen isotope studies of contact metamorphism in the Santa Rosa Range, Nevada and other areas: Contributions to Mineralogy and Petrology, v. 20, p. 306–356. doi:10.1007/BF00373303

Sobolev, A.V., and Chaussidon, M., 1996, H_2O concentrations in primary melts from supra-subduction zones and mid-ocean

ridges: Implications for H_2O storage and recycling in the mantle: Earth and Planetary Science Letters, v. 137, p. 45–55. doi:10.1016/0012-821X(95)00203-O

Stone, W.E., Deloule, E., and Stone, M.S., 2003, Hydromagmatic Amphibole in komatiitic, tholeiitic, and ferropicritic units, Abitibi greenstone belt, Ontario and Quebec: Evidence for Archean wet basic and ultrabasic melts: Mineralogy and Petrology, v. 77, p. 39–65. doi:10.1007/s00710-002-0194-3

Strauss, H., and Beukes, N.J., 1996, Carbon and sulfur isotopic compositions of organic carbon and pyrite in sediments from the Transvaal Supergroup, South Africa: Precambrian Research, v. 79, p. 57–71. doi:10.1016/0301-9268(95)00088-7

Sumner, D.Y., and Bowring, S.A., 1996, U-Pb geochronologic constraints on deposition of the Campbellrand Subgroup, Transvaal Supergroup, South Africa: Precambrian Research, v. 79, p. 25–35. doi:10.1016/0301-9268(95)00086-0

Teigler, B., and Eales, H.V., 1996, The lower and critical zones of the western limb of the Bushveld Complex as intersected by the Nooitgedacht boreholes: Bulletin 111, Council for Geoscience, 126 p.

Thompson, A.B., 1992, Water in the Earth's upper mantle: Nature, v. 358, p. 295–302. doi:10.1038/358295a0

Uken, R., and Watkeys, M.K., 1997, Diapirism initiated by the Bushveld Complex, South Africa: Geology, v. 25, p. 723–726. doi:10.1130/0091-7613(1997)025<0723:DIBTBC>2.3.CO;2

VanTongeren, J.A., 2018, Mixing and unmixing in the Bushveld Complex magma chamber, in Mondal, K., and Griffin, W.L., eds., Processes and ore deposits of ultramafic-mafic magmas through space and time: Chennai, Elsevier, 113–138 p.

VanTongeren, J.A., Zirakparvar, N.A., and Mathez, E.A., 2016, Hf isotopic evidence for a cogenetic magma source for the Bushveld Complex and associated felsic magmas: Lithos, v. 248-251, p. 469–477. doi: 10.1016/j.lithos.2016.02.007

Viljoen, M.J., and Scoon, R.N., 1985, The distribution and main geologic features of discordant bodies of iron-rich ultramafic pegmatite in the Bushveld Complex: Economic Geology, v. 80, p. 1109–1128. doi:10.2113/gsecongeo.80.4.1109

Von Gruenewaldt, G., Sharpe, M.R., and Hatoon, C.J., 1985, The Bushveld Complex: Introduction and review: Economic Geology, v. 80, p. 803–812. doi:10.2113/gsecongeo.80.4.803

Walraven, F., 1988, Notes on the age and genetic relationships of the Makhutso Granite, Bushveld Complex, South Africa: Chemical Geology: Isotope Geoscience Section, v. 72, p. 17–28.

Willmore, C.C., Boudreau, A.E., Spivack, A., and Kruger, F.J., 2002, Halogens of Bushveld Complex, South Africa: δ37Cl and Cl/F evidence for hydration melting of the source region in a back-arc setting: Chemical Geology, v. 182, p. 503–511. doi: 10.1016/S0009-2541(01)00337-0 2-4

Wilson, A.J., 2015, The Earliest Stages of Emplacement of the Eastern Bushveld Complex: Development of the Lower Zone, Marginal Zone, and Basal Ultramafic Sequence: Journal of Petrology, v. 56, p. 347–388. doi:10.1093/petrology/egv003

Wilson, J., Ferré, E.C., and Lespinasse, P., 2000, Repeated tabular injection of high-level alkaline granites in the eastern Bushveld, South Africa: Journal of the Geological Society of London, v. 157, p. 1077–1088.

Woodhead, J., Stern, R.J., Pearce, J., Hergt, J., and Vervoort, J., 2012, Hf-Nd isotope variation in mariana trough basalts: The importance of "ambient mantle" in the interpretation of subduction zone magmas: Geology, v. 40, no. 6, p. 539–542. doi:10.1130/G32963.1

Yang, S.-H., Maier, W.D., Lahaye, Y., and O'Brien, H., 2013, Strontium isotope disequilibrium of plagioclase in the Upper critical zone of the Bushveld Complex: Evidence for mixing of crystal slurries: Contributions to Mineralogy and Petrology, v. 166, p. 959–974. doi:10.1007/s00410-013-0903-4

Zeh, A., Gerdes, A., 2014, HFSE (High Field Strength Elements)-transport and U–Pb–Hf isotope homogenization mediated by Ca-bearing aqueous fluids at 2.04Ga: Constraints from zircon, monazite, and garnet of the Venetia Klippe, Limpopo Belt, South Africa: Geochimica Et Cosmochimica Acta, v. 138, p. 81–100. doi: 10.1016/j.gca.2014.04.015

Zeh, A., Gerdes, A., Will, T.H., and Frimmel, H.E., 2010, Hafnium isotope homogenization during metamorphic zircon growth in amphibolite-facies rocks: Examples from the Shackleton Range (Antarctica): Geochimica Et Cosmochimica Acta, v. 74, p. 4740–4758. doi:10.1016/j.gca.2010.05.016

Zeh, A., Wilson, A.H., Gudelius, D., and Gerdes, A., 2020, Hafnium Isotopic Composition of the Bushveld Complex Requires Mantle Melt–Upper Crust Mixing: New Evidence from Zirconology of Mafic, Felsic and Metasedimentary Rocks. Journal of Petrology. 11 11 60, p. 2169–2200. doi: 10.1093/petrology/egaa004 11

Zhu, G., Gerya, T.V., Yuen, D.A., Honda, S., Yoshida, T., and Connolly, J.A.D., 2009, Three-dimensional dynamics of hydrous thermal-chemical plumes in oceanic subduction zones: Dynamics of 3-D hydrous thermal-chemical plumes: Geochemistry, Geophysics, Geosystems, v. 10.

Zirackparvar, N.A., Mathez, E.A., Scoates, J.S., and Wall, C.J., 2014, Zircon Hf isotope evidence for an enriched mantle source for the Bushveld Igneous Complex: Contributions to Mineralogy and Petrology, v. 168, p. 1050. doi:10.1007/s00410-014-1050-2